Water Air Soil Pollut (2024) 235:602
https://doi.org/10.1007/s11270-024-07364-2

A Study of Copper and Lead Removal from Synthetic Leachate by Photocatalysis

Veena S. Soraganvi · Naveen N. Desai

Received: 25 July 2022 / Accepted: 18 July 2024

Abstract Most undeveloped and developing countries have adopted landfill as the ultimate disposal method for their Municipal Solid Waste (MSW). Leachate produced by a landfill site is highly dangerous, with high concentrations of organic and inorganic pollutants, ammonia and toxic heavy metals. Heavy metals commonly found in landfill leachate are copper, lead, mercury, cadmium, arsenic etc., The main objective of this research is to study the removal of heavy metals copper and lead, from synthetic leachate using TiO_2 and Ag-doped TiO_2 nanomaterials by a heterogeneous photocatalytic process. The photocatalytic experiments were conducted using a compound parabolic collector in sunlight. The design of experiment is used to obtain the minimum number of experiments for the study, to analyze the data and to understand the interaction between the process variables and their responses. Photocatalytic behavior of copper and lead removal has been demonstrated using an Artificial Neural Network (ANN) model. Characterization studies are conducted on TiO_2 and Ag-doped TiO_2 nanomaterials by XRD, SEM and EDX. At optimum parameters of the dosage 0.75 g/L, pH 5 and irradiation time of 100 min, copper removal from synthetic leachate was found to be 80.38% and 80.12%, lead removal efficiency was 97.2% and 96.34% for TiO_2 and Ag-doped TiO_2, respectively. The determination coefficient value obtained by RSM and ANN ensures that the developed model of copper and lead removal gives an accurate prediction. The kinetic study shows that, copper and lead removal by photocatalytic process are described well by a Langmuir–Hinshelwood kinetic model.

Keywords Artificial neural network · Kinetic study · Response Surface Methodology (RSM) · TiO_2 · Ag-doped TiO_2 nanomaterial

1 Introduction

Leachate from a sanitary landfill has a high concentration of organic, inorganic and heavy metals. Sources of heavy metals in MSW include, electronic items, used batteries, painting waste, fluorescent tubes, and photographic chemicals (Boateng et al., 2019). These heavy metals enter in the soil, surface water and groundwater through leaching and their toxicity can cause serious problems in environment, human health and are non-biodegradable. Heavy metals can remain in landfill for about 150 years, and leaches at a rate of

V. S. Soraganvi (✉) · N. N. Desai
Department of Civil Engineering, Basaveshwar Engineering College, Bagalkot 587103, Karnataka, India
e-mail: veena_snv@yahoo.co.in; vsscv@becbgk.edu

N. N. Desai
e-mail: desainaveen16@gmail.com

N. N. Desai
Department of Civil Engineering, B.L.D.E.A's V.P. Dr P.G.Halakatti. College of Engineering & Technology, Vijayapur 586103, Karnataka, India

Published online: 13 August 2024

400 mm/year (Hussein et al., 2021). Traces of heavy metals such as cadmium (Cd), mercury (Hg), arsenic (As), chromium (Cr) and lead (Pb) can have toxic effects on the human body through food and drinking water. (Ali et al., 2021).

Conventional treatment techniques such as physical, chemical or biological in individual or in integrated sequence are not feasible for leachate treatment because biological treatment is effective in treating young leachate (<5 years) and their performance decrease for mature landfill (>10 years) (Bandala et al., 2021). The conventional method of leachate trexatment does not work completely to remove pollutants from the leachate in order to meet the discharge standards limits (Show et al., 2019). Now days heterogeneous photocatalysis has been found to be most promising tool in wastewater treatment because it uses semiconductor nanomaterials as a photocatalyst, oxygen as oxidizing agent, water as the solvent and artificial light or solar light as the irradiation source. So it is universally recognized as a green and inexpensive technology (Parrino et al., 2018). Ferric oxides, aluminum oxides, titanium oxides, manganese oxides, and magnesium oxides are different semiconductor nanomaterials used in the heterogeneous photocatalysis. Among these semiconductor nanomaterials, TiO_2 nanomaterial has gained a prominence due to its non-toxicity, cost-effectiveness, high chemical stability, and its high oxidizing power, making it a competitive candidate for many photocatalytic applications (Desai & Soraganvi, 2019).

The removal of heavy metals in the UV and visible range with artificial lamps and solar light were performed in aqueous solution using different semiconductor nanomaterials by many researchers (Sobhanardakani et al., 2018; Zangeneh et al., 2018; Zhao & Wu, 2018). Applicability of TiO_2 and Ag doped TiO_2 nanomaterial on removal of heavy metals from young leachate in natural sunlight is not performed. The present study deals with the removal of copper and lead from synthetic leachate by photocatalysis in natural sunlight using a compound parabolic collector (CPC). The selection of copper and lead for removal in this study is based on their significant presence in leachate from sanitary landfills. These heavy metals, originating from electronic items, used batteries, painting waste, fluorescent tubes, and photographic chemicals in municipal solid waste (MSW), pose serious environmental threats. When leachate containing copper (Cu) and lead (Pb) leaches into the soil, surface water, and groundwater, it can have adverse effects on both the environment and human health. Copper and lead are known to be non-biodegradable and can persist in landfills for extended periods, with leaching rates contributing to potential contamination at a rate of 400 mm/year. The toxic effects of trace amounts of these heavy metals on humans through food and drinking water have been well-documented (Li et. al., 2023). Hence, the removal of copper and lead from synthetic leachate becomes a crucial area of investigation in the context of environmental protection and waste management.

Design of experiment had been used in this study to improve the reliability of the experimental results and study of effect of more than one parameter at a time. TiO_2 and Ag-doped TiO_2 nanomaterial characterization is performed and the effect of each factor on the removal of copper and lead from synthetic leachate is studied by three-dimensional surface plots and contour maps from the RSM. Further, inputs of pH, dosage and irradiation time and output as a percentage of copper and lead removal are used in ANN, to predict the copper and lead removal efficiency. The Langmuir–Hinshelwood (L–H) model is used to study the reaction rate of the experiments in removal of copper and lead. The experiments were performed in Bagalkot, Karnataka State of India.

2 Materials and Methodology

2.1 Preparation of Synthetic Leachate

The landfill is categorized into four phases in its life course, which are; aerobic, anaerobic acid phase, initial methanogenic phase and stable methanogenic phase. The young landfill leachate is produced in the anaerobic acid phase; in which the leachate is capable of dissolving the metal ions in it, leading to the high concentration of heavy metals in the leachate (Kanmani & Gandhimathi, 2013). Therefore, heavy metals are usually found in higher concentrations in young leachates. In nearby disposal site we could not find any leachate with high metals concentration. Therefore, in the present study synthetic leachate is prepared in accordance with the equivalent characteristics of young leachate with high COD, high metal concentration, nitrate, chloride etc., and

removal of copper and lead were studied independently. The prepared synthetic leachate for the study has not been inoculated with bacteria cultivation, so no biodegradability study has been conducted. It was observed that lead is significantly suppressed by fluoride, iodide, carbonate and phosphate, so dipotassium phosphate and potassium carbonate chemicals are not added in the synthetic leachate preparation for lead (Herrmann & Bucksch, 2014). But same are added in the synthetic leachate of copper. The synthetic leachate is prepared by dissolving the analytical grade chemicals in deionized water as shown in Table 1 (Champagne & Li, 2009; Mohan & Gandhimathi, 2009).

2.2 Synthesis of Silver Doped TiO_2 Nanoparticles

Silver doped TiO_2 reduces the energy band gap, which is the energy needed to move an electron from the valence band to the conduction band of the catalyst, producing photogenerated holes on the surface of the catalyst. Moreover, the presence of noble metals can reduce the phenomenon of recombination between electron–hole pairs due to the scavenging of photogenerated electrons (Gomes et al., 2018).

TiO_2 nanomaterial purchased from Sisco Research Laboratories Pvt. Ltd (SRL)-India is used in this study. The "Sol–gel method" was used to dope silver on Titanium dioxide. 4 gms of TiO_2 was taken into a 500 ml pyrex beaker, containing 100 ml of deionized water. For Ag doping, 1% (molar ratio) of $AgNO_3$ was added to the suspension and stirred vigorously with a magnetic stirrer for 30 min and then left undisturbed at room temperature (25–30^0 C) overnight. The liquid was then dried for 12 h at 100 °C in a hot air oven, to remove the remaining moisture content. Later the residue was calcinated for 3 h in a muffle furnace at 500 °C. Finally, mortar and pestle are used to grind the sample, to get fine particles. The resulted fine particles were Ag-TiO_2 nanoparticles (Ilyas et al., 2011; Kulkarni et al., 2016).

2.3 Mechanism of Heavy Metal Removal by Photocatalysis

Heterogeneous photocatalysis, a powerful advanced oxidation process (AOP), relies on the utilization of semiconductor nanomaterials, such as TiO_2 and Ag-doped TiO_2 as used in this study, as efficient photocatalysts. These semiconductor nanomaterials possess a characteristic bandgap energy (E_g), which represents the energy difference between their valence band and conduction band. When these photocatalysts are exposed to light with energy equal to or greater than the bandgap energy, they undergo excitation, resulting in the generation of electron–hole pairs. Upon photon absorption, electrons in the valence band gain sufficient energy to move to the higher energy conduction

Table 1 Composition of synthetic leachate for copper and lead

Sl.No	Constituents	Per litre of synthetic leachate	
		For copper	For lead
1	Copper sulphate –$Cu(SO_4)_2$	3920 mg	–-
2	Lead Nitrate –$Pb(NO_3)_2$	–-	1599 mg
3	Potassium bicarbonate -$KHCO_3$	312 mg	312 mg
4	Dipottassium phosphate -K_2HPO_4	30 mg	–-
5	Sodium nitrate -$NaNO_3$	50 mg	50 mg
6	Potassium carbonate -K_2CO_3	324 mg	–-
7	Calcium chloride dihydrate -$CaCl_2.2H_2O$	2882 mg	2882 mg
8	Sodium bicarbonate -$NaHCO_3$	3012 mg	3012 mg
9	Magnesium sulphate -$MgSO_4$	156 mg	156 mg
10	Magnesium chloride hexahydrate -$MgCl_2.6H_2O$	3114 mg	3114 mg
11	Urea -$CO(NH_2)_2$	695 mg	695 mg
12	Ammonium bicarbonate -NH_4HCO_3	2439 mg	2439 mg
13	Acetic acid (99%)	7 ml	7 ml
15	Propionic acid	5 ml	5 ml
16	Sodium hydroxide (1N)	For adjusting pH	For adjusting pH

band, leaving behind positively charged holes in the valence band. This process of excitation and charge separation creates photogenerated electrons (e-) in the conduction band and positive holes (h+) in the valence band, which play pivotal roles in the photocatalytic reactions (Spasiano et al., 2015).

The photogenerated electrons (e-) in the conduction band act as potent reducing agents. Specifically, in the context of heavy metal removal from synthetic leachate, these electrons can effectively reduce metal ions (M^n+) present in the wastewater (Gopinath et al., 2020; Litter, 2015). Consequently, the reduced metal ions ($M^{(n-1)}+$) exhibit a lower oxidation state compared to their original form, making them less toxic and more amenable to immobilization or precipitation. Simultaneously, the positive holes (h+) in the valence band possess strong oxidative properties. These holes drive the oxidation of various organic compounds present in the synthetic leachate, breaking them down into simpler and less harmful compounds. The ultimate result is the mineralization of these organic pollutants into carbon dioxide (CO_2) and water (H_2O).

Apart from the photogenerated electron–hole pairs, oxygen molecules (O_2) present in the system play a crucial role in the photocatalytic process. Some of the photogenerated electrons (e-) in the conduction band react with oxygen molecules, generating superoxide radicals ($O2^{\bullet-}$) and other reactive oxygen species. These reactive oxygen species further participate in oxidation reactions, contributing to the effective degradation of organic pollutants (Spasiano et al., 2015). The surfaces of semiconductor nanomaterials also play a significant role in photocatalysis. Due to their high surface area and surface charge characteristics, these materials can adsorb organic compounds and metal ions, leading to enhanced interactions between the photocatalysts and the pollutants. This surface adsorption process can further improve the efficiency of degradation and removal processes. These photogenerated electrons and positive holes bring about reduction and oxidation respectively as shown in Fig. 1.

$$M^{n+} + ne \rightarrow M \tag{1}$$

In some cases, sacrificial agents like methanol or formaldehyde may be introduced to enhance the reduction reactions. These sacrificial agents react with the photogenerated positive holes, regenerating the valence band and enabling prolonged photocatalytic activity.

$$RCH_2OH + HO^{\bullet} \rightarrow {}^{\bullet}RCHOH + H_2O \tag{2}$$

$$M^{n+} + {}^{\bullet}RCHOH \rightarrow M^{(n-1)+} + RCHO \tag{3}$$

It is also possible for the metallic ions to get oxidize by pores or $HO^{\bullet}$, by reaching a higher oxidation state. Where 'R' is the alkyl group.

$$M^{n+} \xrightarrow{h^+_{VB}/HO^{\bullet}} M^{n+1} \tag{4}$$

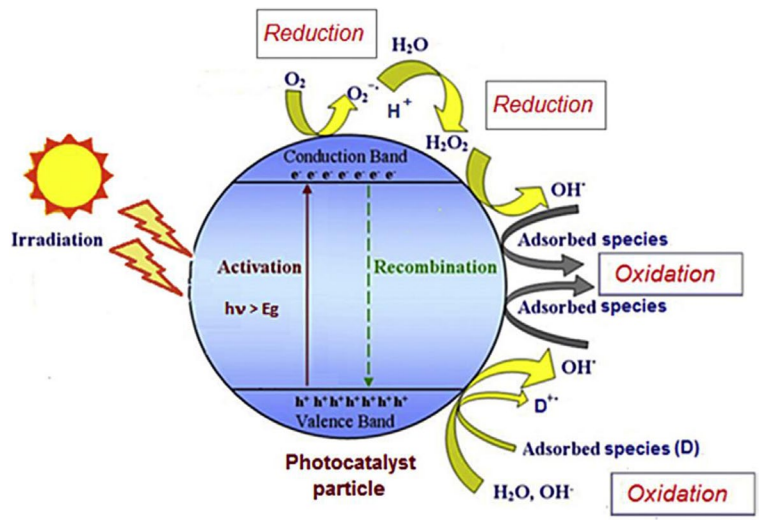

Fig. 1 Heterogeneous photocatalytic process (Spasiano et al., 2015)

2.4 Experimental Study

All the photocatalysis experiments were carried out in September and October in north Karnataka where the average solar radiation is found to be 4.28 kWh/m^2/day and 5.29 kWh/m^2/day respectively for these two months. The CPC profile is prepared in an AutoCAD software by taking two halves of the parabola with closely located focal points and their axis inclined to each other (Strauss et al., 2018; Tanveer & Tezcanli, 2013). The height of the CPC, the width of the receiver and the width of the absorber are 417.5, 360 and 100 mm respectively. As shown in Fig. 2, aluminium foil is used on the reflected surface to collect maximum photons from the sun.

The 1:100 diluted synthetic leachate is added with hole scavenger; EDTA for copper and citric acid for the lead. The TiO_2 nanomaterial is added in suspension form and stirred magnetically in the dark for 30 min to attain adsorption and desorption equilibrium between the leachate and TiO_2. The leachate was taken to CPC reactor for photocatalysis experiment by sunlight and recirculated through the glass cylinder with the aid of a low rpm water pump maintaining a uniform flow rate of 1000 ml/minute. After treatment, the solution is filtered through a 0.45 µm membrane filter paper. Copper and lead concentration were measured with the Varian AAS 240. The pH was measured with a Systronics Make 361pH meter.

The photocatalysis utilizes less amount of chemicals and no waste sludge is produced during the process (Lin et al., 2020). Therefore, sludge analysis is not performed in this study.

Fig. 2 CPC of reflective surface covered with aluminum foil

2.5 Central Composite Design (CCD)

The DESIGN EXPERT 11 (Stat-Ease Inc., Minneapolis, MN, USA) software is used to study the individual and synergetic effects of three factors: pH, dosage and irradiation time to study the performance of removal of copper and lead from the synthetic leachate. The factors are coded as + 1 and -1 for high and low values for the parameters. The range of high and low variables was decided based on literature and presented in Table 2. Rresponse values obtained from the CCD and percentage removal of copper and lead against each experiment are shown in Table 3.

2.6 Artificial Neural Network (ANN)

ANN is a multi-layer fully connected neural nets as shown in Fig. 3. It consists of three layers consisting of input, hidden and output layers. The present study is conducted with back-propagation, and it helps to obtain minimum error by altering the values of weight in training data. To get a better overview, the data in network points are arbitrarily divided into three subsets that contain 70%, 15% and 15% of data. The first subsets are employed for training while the other two subsets are employed for validation and cross-validation (Jin et al., 2002; Haykin, 2014). The weights

Table 2 Experimental factors and levels in the central composite design

Factors	Levels			Star point α = 2	
	Low	Central	High	-α	+α
(X_1) pH	3	5	7	1.634	8.363
(X_2) dosage (gm/L)	0.5	0.75	1	0.329	1.170
(X_3) irradiation time (min)	50	100	150	15.910	184.09

Table 3 Data statistics of model variables

Run	X_1:pH	X_2:Dosage in gm/L	X_3:irradiation time in minutes	Copper removal by TiO_2 in %	Copper removal by Ag-doped TiO_2 in %	Lead removal by TiO_2 in %	Lead removal by Ag-doped TiO_2 in %
1	5	0.75	100	74.12	76.04	98.75	97.89
2	3	0.5	150	58.83	56.28	78.53	75.23
3	5	0.75	100	80.38	79.18	97.65	97.35
4	5	0.75	100	75.13	75.12	96.45	96.16
5	7	0.5	50	35.49	35.83	98.12	99.34
6	5	0.33	100	31.68	52.71	94.16	91.02
7	3	1	150	84.41	55.04	87.52	84.69
8	5	0.75	100	77.16	77.92	97.2	95.34
9	5	0.75	100	81.43	75.17	98.12	97.32
10	3	0.5	50	34.81	17.13	74.32	70.32
11	5	1.17	100	44.56	66.57	98.89	99.43
12	5	0.75	100	75.35	80.12	96.35	96.34
13	5	0.75	16	49.48	49.68	92.12	90.36
14	2	0.75	100	59.73	12.13	66.49	61.67
15	3	1	50	27.75	19.65	81.13	78.76
16	8	0.75	100	35.14	45.23	100	100
17	7	1	50	28.26	54.97	98.87	98.68
18	7	0.5	150	41.37	60.25	98.2	98.45
19	5	0.75	184	96.32	99.02	99.57	99.05
20	7	1	150	48.44	77.16	99.34	98.47
Standard Deviation (SD)				3.77	1.81	1.52	1.53
Mean				56.99	58.26	92.59	91.29
Standard error				0.8430	0.4047	0.3399	0.3421
Coefficient of variation (C.V%)				6.62	3.11	1.64	1.68

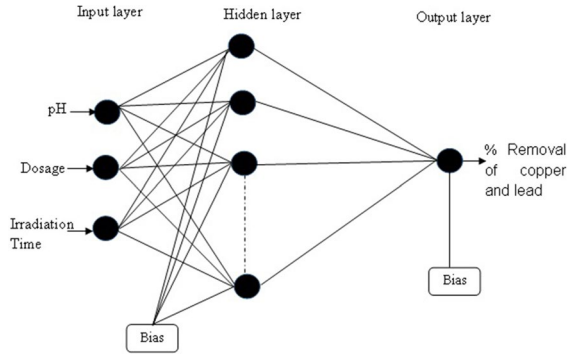

Fig. 3 Artificial neural network

before the training are random with no meaningful information, but after the training contain meaningful information. The input variables examined for the ANN modeling were pH, catalyst dosage and irradiation time. The target value is the percentage removal of heavy metals copper and lead from the leachate.

2.7 Kinetic Study

The adsorption kinetic study is also performed as it helps in obtaining optimum conditions of metal removal, indicating better knowledge of possible rate-controlling steps and mechanism of sorption. The adsorption kinetics are of pseudo-first and pseudo-second-order kinetics which is applied on adsorption data (Batool et al., 2018). Adsorption of pollutants on the semiconductor surface is a significant parameter in heterogeneous photocatalysis.

Expression of Langmuir–Hinshelwood (LH) kinetics expression used for the study is shown in Eq. 5 (Subramonian et al., 2017).

$$\ln\left(\frac{C}{C_0}\right) = -K_{app}t \quad (5)$$

where C (mg/L) is a concentration of pollutants at any time t after beginning of the experiment, and C_0 is the initial concentration of pollutants in the leachate in mg/L and t is the irradiation time in minutes. The apparent rate constant $\left(K_{app}\right)$ can be determined by plotting $\ln(\frac{C_0}{C})$ versus t and obtaining slope of the straight-line plots.

3 Results and Discussion

3.1 Characterization Study of Synthetic Leachate

The physicochemical characteristics of the synthetic leachate are analysed according to the American Public Health Association (APHA, 1999) and the results are presented in Table 4. Table 4 contains characteristics of young landfill leachate to compare with synthetic leachate. Synthetic leachate of copper has a strong blue colour due to the blue crystalline solids of cupric nitrate and synthetic leachate of Lead is a colourless solution.

The pH of the synthetic leachate was found to be 3.34 and 3.12 for copper and lead respectively. This is due to the addition of acetic acid, and propionic acid. The K_2HPO_4 releases the phosphorus to the synthetic leachate for the Copper with the value of 19 mg/L but is absent in the synthetic leachate of Lead. The value of nitrate in the synthetic leachate of lead (291 mg/L) is higher compared to that of copper (38 mg/L), as lead nitrate is being used for heavy metal content identification. Similarly, the value of sulphate is more in the synthetic leachate for copper (523 mg/L) compared to that of lead (480 mg/L) due to the addition of copper sulphate. The total dissolved solids present in the synthetic leachate of copper and lead are 9300 mg/L and 11,300 mg/L, respectively. The results obtained for TDS, chloride, calcium and magnesium are in line with the previous works conducted on synthetic leachate (Rosin-Paumier et al., 2011).

The prepared leachate has concentration of 1000 mg/L of copper/lead, which is reduced to 8.2 ± 0.3 mg/L when diluted to 1:100 for the purpose of the reduction study.

3.2 Characterization Study TiO_2 and Ag-doped TiO_2

3.2.1 Scanning Electron Microscope (SEM) Analysis

SEM images of TiO_2 and Ag-doped TiO_2 nanoparticles were carried out under different magnifications. Figure 4(a) shows the SEM images of TiO_2. It is observed that there is a dense agglomeration of

Table 4 Physicochemical characteristics of synthetic leachate

Parameters	Values of synthetic leachate for copper	Values of synthetic leachate for lead	Standards of young landfill Leachate [43, 44] Range [43, 44]
Temperature (^{0}C)	28.00	27.20	--
pH	3.34	3.12	4.5–7.5
Electrical Conductivity (µs/cm)	19,000	23,200	2500–35000
Total dissolved Solids (mg/L)	9300	11,300	2000–60000
COD (mg/L)	17,386	17,512	6000–60000
Calcium (mg/L)	1132	960	10–2500
Magnesium (mg/L)	398	336	50–1150
Chloride (mg/L)	3600	5000	150–4500
Sulphates (mg/L)	523	480	70–1750
Phosphorus (mg/L)	19	---	0.1–23
Nitrate (mg/L)	38	291	---
Copper (mg/L)	1000	---	0.005–10
Lead (mg/L)	---	1000	0.001–5

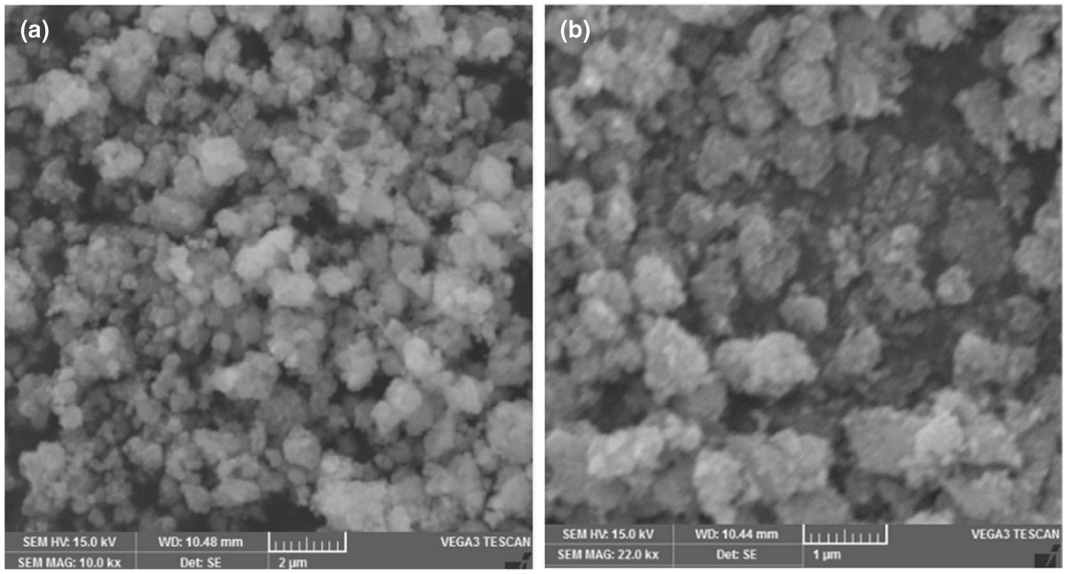

Fig. 4 **a** TiO_2 SEM images. **b** Ag doped TiO_2 SEM images

particles due to the high surface to volume ratio of nanoparticles. The high surface free energy needs to be diminished, therefore particles will get agglomerated. The shape of the particles is not uniform and look like spherical.

Figure 4(b) shows SEM images of Ag-doped TiO_2, the distribution of silver on the surface of TiO_2 is non-uniform and Ag-doped TiO_2 contains irregularly shaped particles because of the aggregation of minute crystals. SEM results show that doping with silver leaves no change in the topology of the catalyst surface. The Surface area of particles seems spongy and porous structure at high hardness, which favors the photocatalytic applications and absorption (Sarteep et al., 2016).

3.2.2 X-Ray Diffraction (XRD) Analysis

XRD analysis, is used to study the crystal structure, to identify the crystalline phases present in a material and thereby reveal chemical composition information. XRD spectra of TiO_2 and doped TiO_2 are shown in Fig. 5(a) and (b). Data were collected for the 2θ values between 10° to 90° with a scanning rate of 0.02° per second.

TiO_2 and Ag-doped TiO_2 peak values were compared and Ag-doped TiO_2 has greater peak values at 25.43^0, 38.70^0 and 48.18^0 compared to TiO_2, indicating a sign of decreased particle size in doped TiO_2 (Zangeneh et al., 2018).

The crystallite size (D) can be calculated from the Full width half maximum (FWHM) using XRD peaks with Scherer's equation (Eq. 6). Calculation of particle size using Debye-Scherer equation

$$D = \frac{k\lambda}{\beta cos\theta} \tag{6}$$

where D is crystallite size (nm), k is constant, λ is X-ray wavelength (0.15406), β is the corrected FWHM in radian and θ is Bragg angle.

The calculated crystallite size for pure and doped TiO_2 has been found to be 19.29 nm and 15.36 nm respectively. Results of our study agree with previous works, where 14.17 nm and 13.07 nm were reported for 1% and 2% of Ag-doped TiO_2 (Kulkarni et al., 2016).

With the XRD technique, crystallographic phases of TiO_2 and Ag-doped TiO_2 nanoparticles are identified. The XRD spectra for TiO_2 in Fig. 5(a) shows 2θ peak at 25.39^0, 37.95^0 and 62.82^0 corresponding to the planes (101), (103), and (204) which confirms that the TiO_2 is anatase according to JCPDS card no.71–1169. For the Ag-doped TiO_2 nanoparticles Fig. 5(b) shows 2θ peaks at 25.43^0, 37.91^0, 48.18^0,

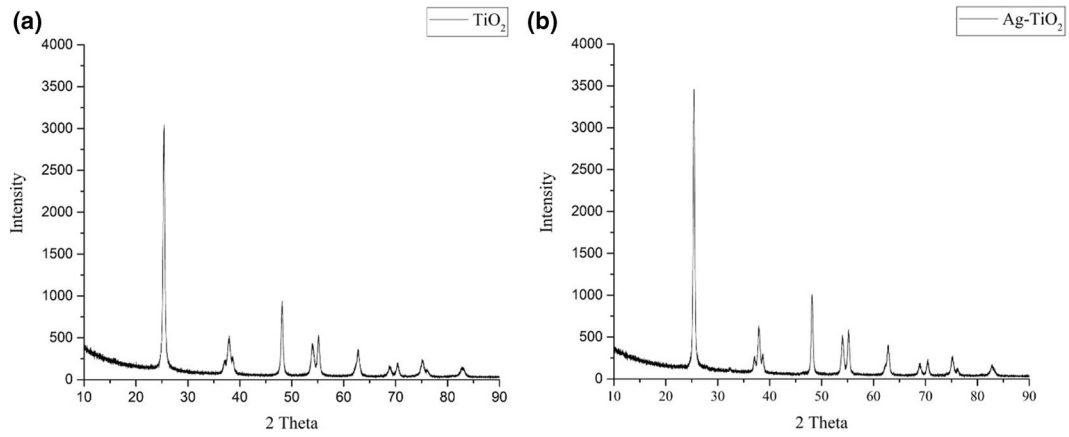

Fig. 5 **a** TiO_2 XRD graph. **b** Ag-doped TiO_2 XRD graph

53.99^0 and 62.79^0 corresponding to the planes (101), (004), (200), (105) and (204) which confirms that the TiO_2 is also of anatase form according to (JCPDS card no. 84–1285). It is observed that the main anatase peak of (101) plane shifted from 25.39° to 25.43° due to doping of TiO_2 with silver.

3.2.3 Energy Dispersive X- ray Spectroscopy (EDX)

EDX provides data with the ratio of the element at the surface of the composite. The EDX data were collected at different spectrum at 1, 2 and 3 for the TiO_2. Figure 6(a) shows Ti and O peaks only, no other peak for any other elemental has been reported in the spectrum. This confirms that the nanoparticles used for the study is TiO_2. The collected data from different spectrum indicates the atomic % of Ti and O value. Figure 6(a) shows that the Ti composition is 17.08 and O as 82.92 in atomic %.

EDX pattern of Ag-doped TiO_2 nanomaterial are shown in Fig. 6(b) these confirm the presence of Ag, Ti and O. The sample is analyzed at low accelerating voltage, therefore it is possible to get Ag L peak alone and Ag K peak was absent. The peaks from the spectrum show the presence of O, Ag and Ti at 0.5, 3 and 4.5 keV respectively. Further, the atomic % is analyzed and found the values of Ti, O, and Ag as 20.65, 78.35 and 1 respectively. The combination of Ti, O and trace amounts of Ag offers better photocatalytic activity compared to TiO_2.

3.3 Statistical Analysis for Model Verification

The removal of copper and lead from the synthetic leachate were carried out according to the CCD chart for TiO_2 and Ag-doped TiO_2 and results are listed in

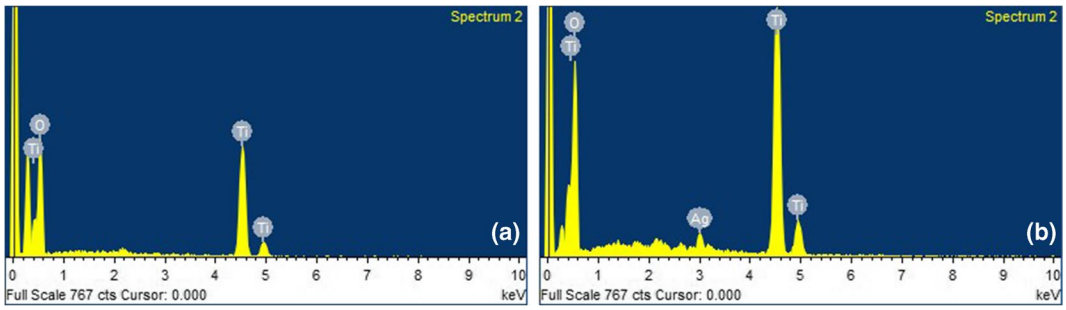

Fig. 6 **a** EDX analysis of TiO_2. **b** EDX analysis of Ag- doped TiO_2

Table 3. Analysis of variance (ANOVA) is a method used to evaluate the individual interface and quadratic effects of the variables influencing the percentage removal of copper and lead from synthetic leachate. Various models such as linear, 2 FI and cubic have been studied, but the quadratic polynomial model has been found to be suitable for the removal of copper and lead from the synthetic leachate. The results of the regression equations with coded variables for copper and lead with respect to TiO_2 and Ag-doped TiO_2 are presented in Eqs. (7), (8), (9), and (10). The below-coded equation helps in predicting the response for given levels of each factor.

$$\text{Copper removal by } TiO_2(\%) = 77.47 - 6.85X_1 + 2.93X_2 + 13.58X_3 - 2.33X_1X_2 - 6.83X_1X_3 + 5.87X_2X_3 - 11.90X_1^2 - 15.19X_2^2 - 2.90X_3^2 \quad (7)$$

$$\text{Copper removal by Ag} - \text{doped } TiO_2(\%) = 77.45 - 9.94X_1 + 4.44X_2 + 14.97X_3 + 4.35X_1X_2 - 3.49X_1X_3 - 0.7487X_2X_3 - 18.40X_1^2 - 7.46X_2^2 - 2.22X_3^2 \quad (8)$$

$$\text{Lead removal by } TiO_2(\%) = 97.47 + 9.86X_1 + 1.88X_2 + 1.73X_3 - 1.74X_1X_2 - 1.26X_1X_3 + 0.321X_2X_3 - 6.53X_1^2 - 0.466X_2^2 - 0.709X_3^2 \quad (9)$$

$$\text{Lead removal by Ag} - \text{doped } TiO_2(\%) = 96.76 + 11.47X_1 + 2.30X_2 + 1.78X_3 - 2.32X_1X_2 - 1.49X_1X_3 + 0.2152X_2X_3 - 7.20X_1^2 - 0.620X_2^2 - 0.804X_3^2 \quad (10)$$

Further ANOVA is used to verify the adequacy of the developed polynomial models for copper and lead in terms of coefficient of determination R^2, p-value and F-value (Varank et al., 2016).

For TiO_2 and Ag-doped TiO_2, the developed models of copper and lead are significant or insignificant, is studied with the relationship between predicted and actual data as shown in Fig. 7(a) and (b) for the copper and Fig. 8(a) and (b) for the lead. The predicted R^2 value for the copper with respect to TiO_2 and Ag-doped TiO_2 were found to be 0.8324 and 0.9177 respectively: and for the lead it is 0.9245 and 0.9403 respectively. The obtained predicted R^2 values for copper and lead are in reasonable agreement with the adjusted R^2 value of copper 0.9521 and 0.9757 and lead 0.9760 and 0.9813 respectively, as the difference is less than 0.2. Therefore, the model obtained by ANOVA is significant for both the copper and lead removal. The R^2 value of lead was found to be higher compared to copper, because lead model explains maximum variability of the response data around its mean. The large value of R^2 does not prove that the model is good, because it describes the goodness of fit of the linear regression models, therefore it is verified further in terms of F-value, p-value and adequate precision.

The sum of squares, mean square of each factor, F-values and p—values are shown in Table 5 for the copper and Table 6 for the lead with respect to TiO_2 and Ag-doped TiO_2. For the percentage removal of copper, the Model F-value of TiO_2 and Ag-doped TiO_2 is 4.08 and 4.84 respectively (for lack of fit). The model F- value for the percentage removal of

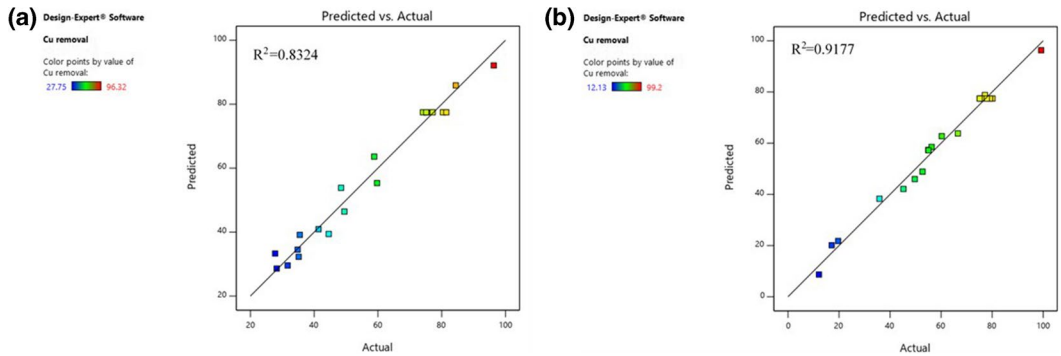

Fig. 7 **a** Predicted and experimental data for % copper removal byTiO_2. **b** Predicted and experimental data for % copper removal by Ag-doped TiO_2

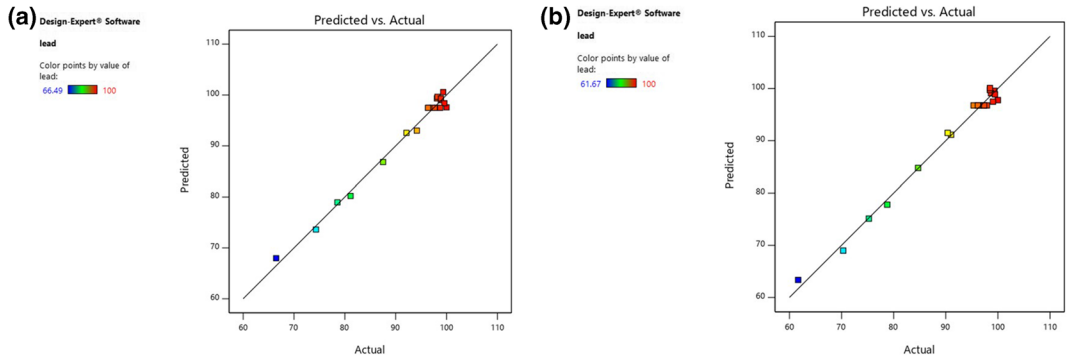

Fig. 8 **a** Predicted and experimental data for % lead removal by TiO_2. **b** Predicted and experimental data for % lead removal by Ag-doped TiO_2

Table 5 The ANOVA for response surface quadratic model for copper removal by TiO_2 and Ag- doped TiO_2

TiO_2						
Source	Sum of squares	Degree of freedom	Mean square	F-value	*p*-value	Remarks
Copper model	8871.40	9	985.71	42.93	< 0.0001	significant
X_1-pH	641.44	1	641.44	27.93	0.0004	significant
X_2-Dosage	117.28	1	117.28	5.11	0.0474	significant
X_3-Irradiation time	2520.04	1	2520.04	109.75	< 0.0001	significant
X_1X_2	43.62	1	43.62	1.90	0.1982	not significant
X_1X_3	372.92	1	372.92	16.24	0.0024	significant
X_2X_3	275.42	1	275.42	11.99	0.0061	significant
X_1^2	2040.50	1	2040.50	88.86	< 0.0001	significant
X_2^2	3326.31	1	3326.31	144.86	< 0.0001	significant
X_3^2	120.86	1	120.86	5.26	0.0447	significant
Residual	229.62	10	22.96			
Lack of Fit	184.44	5	36.89	4.08	0.0744	not significant
Ag-doped TiO_2						
Copper model	10,274.62	9	1141.62	85.93	< 0.0001	significant
X_1-pH	1349.91	1	1349.91	101.61	< 0.0001	significant
X_2-Dosage	269.25	1	269.25	20.27	0.0011	significant
X_3- Irradiation time	3060.19	1	3060.19	230.35	< 0.0001	significant
X_1X_2	151.12	1	151.12	11.38	0.0071	significant
X_1X_3	97.51	1	97.51	7.34	0.0220	significant
X_2X_3	4.49	1	4.49	0.3376	0.5741	Not significant
X_1^2	4880.68	1	4880.68	367.38	< 0.0001	significant
X_2^2	801.36	1	801.36	60.32	< 0.0001	significant
X_3^2	71.31	1	71.31	5.37	0.0430	significant
Residual	132.85	10	13.29			
Lack of Fit	110.11	5	22.02	4.84	0.0542	not significant

Table 6 The ANOVA for response surface quadratic model for lead removal by TiO_2 and Ag- doped TiO_2

TiO_2						
Source	Sum of squares	Degree of freedom	Mean square	F-value	*p*-value	Remarks
Lead model	1784.40	9	198.27	86.97	< 0.0001	significant
X_1-pH	1216.13	1	1216.13	533.46	< 0.0001	significant
X_2-Dosage	48.14	1	48.14	21.12	0.0010	significant
X_3-Irradiation time	41.05	1	41.05	18.01	0.0017	significant
X_1X_2	24.19	1	24.19	10.61	0.0086	significant
X_1X_3	12.63	1	12.63	5.54	0.0404	significant
X_2X_3	0.8256	1	0.8256	0.3622	0.5607	Not significant
X_1^2	438.12	1	438.12	192.18	< 0.0001	significant
X_2^2	3.15	1	3.15	1.38	0.2667	Not significant
X_3^2	7.27	1	7.27	3.19	0.1044	Not significant
Residual	22.80	10	2.28			
Lack of Fit	18.35	5	3.67	4.13	0.0729	Not significant
Ag-doped TiO_2						
Copper model	2359.83	9	262.20	111.49	< 0.0001	significant
X_1-pH	1645.89	1	1645.89	699.83	< 0.0001	significant
X_2-Dosage	72.21	1	72.21	30.70	0.0002	significant
X_3-Irradiation time	43.42	1	43.42	18.46	0.0016	significant
X_1X_2	42.97	1	42.97	18.27	0.0016	significant
X_1X_3	17.82	1	17.82	7.58	0.0204	significant
X_2X_3	0.3612	1	0.3612	0.1536	0.7033	Not significant
X_1^2	532.05	1	532.05	226.23	< 0.0001	significant
X_2^2	5.57	1	5.57	2.37	0.1549	Not significant
X_3^2	9.37	1	9.37	3.98	0.0739	Not significant
Residual	23.52	10	2.35			
Lack of fit	19.03	5	3.81	4.24	0.0694	Not significant

lead by TiO_2 and Ag-doped TiO_2 are found to be 4.13 and 4.24 respectively. These F values suggest that the Lack of Fit is not significant compared to the pure error. Therefore, non-significant lack of fit is suggested to be good for the model.

The model terms with values of p less than 0.05 are considered as significant and same is indicated in the remarks column of Table 5 for copper and Table 6 for the lead. The p-values less than 0.05 for the copper with respect to TiO_2 observed that the linear coefficients (X_1, X_2, X_3) quadratic term coefficients (X_1^2, X_2^2, X_3^2) and cross product coefficients (X_1X_3, X_2X_3) are significant models terms. From the Table 6 for the lead removal by TiO_2, it is observed that linear coefficients (X_1, X_2, X_3) a quadratic term coefficients (X_1^2) and cross product coefficients (X_1X_2, X_1X_3) are significant model terms. Similarly, from Table 5 for removal of copper from Ag-doped TiO_2 significant model terms for linear coefficients are (X_1, X_2, X_3), cross product coefficients are (X_1X_2, X_1X_3) and quadratic term coefficients are (X_1^2, X_2^2, X_3^2). For the lead removal with respect to Ag-doped TiO_2 from the Table 6 significant model terms are linear coefficients (X_1, X_2, X_3), cross product coefficients (X_1X_2, X_1X_3) and quadratic term coefficients (X_1^2). The other terms such as X_1X_2 in TiO_2 and X_2X_3 in Ag-doped TiO_2 are not significant for the copper removal; where as for the lead, insignificant terms are X_2X_3, X_2^2 *and* X_3^2 for the TiO_2 and X_2X_3, X_2^2 *and* X_3^2 for the Ag-doped TiO_2 as corresponding p values are greater than 0.05. These insignificant terms can be removed from the model.

For a model to be significant the adequate precision ratio should be more than 4. In the present study for copper removal using TiO_2 and Ag-doped TiO_2 adequate precision ratio are 18.74 and 34.01 respectively. For the lead it was found to be 18.74 and 33.86 for TiO_2 and Ag-doped TiO_2 respectively. From the statistical results attained and discussed, it is found that the copper and lead models obtained in the Eqs. (3), (4), (5) and (6) are adequate to predict the copper and lead removal from the leachate within the applied range of variables.

3.4 Artificial Neural Network (ANN) Modelling

From the statistical study it is confirmed that, the model obtained from ANOVA in RSM (Eqs. 7, 8, 9 and 10) are adequate to predict the percentage removal of copper and lead within the applied range of variables. To obtain best ANN structure, correlation coefficient R with maximum and MSE with the minimum value were taken for training and test data sets.

The network is trained by varying hidden neurons with 2 to 10 as shown in Table 7 for the copper with respect to TiO_2 and Ag-doped TiO_2, and similarly for lead is as shown in Table 8. The optimized hidden neurons for copper removal by TiO_2 and Ag-doped TiO_2 are found to be 10 and 6 with overall R value of 0.9958 and 0.9968 respectively. For the lead removal by TiO_2 and Ag-doped TiO_2 the same are found to be 2 and 6 with overall R values of 0.9958 and 0.9966 respectively. These neuron results were used to generate the predicted values by ANN for copper and lead removal by TiO_2 and Ag-doped TiO_2.

Table 7 Hidden neuron layers efficiency for copper reduction by TiO_2 and Ag- doped TiO_2

TiO_2					
Number of neurons	Training MSE	Test MSE	Training R	Test R	All R
2	26.0802	61.044	0.9740	0.9984	0.9706
4	2.4433	14.7928	0.9983	0.9940	0.9816
6	2.1219	11.6189	0.9977	0.9982	0.9946
8	1.8274	12.997	0.9981	0.9991	0.9910
10	1.6285	9.0926	0.9982	0.9991	0.9958
Ag-doped TiO_2					
2	16.1355	8.7552	0.9821	0.9800	0.9875
4	1.7000	2.2335	0.9985	0.9990	0.9982
6	0.6473	1.4012	0.9994	0.9991	0.9968
8	1.2100	17.0621	0.9987	0.9860	0.9884
10	2.0666	28.5901	0.9981	0.9987	0.9921

Table 8 Hidden neuron layers efficiency for lead reduction by TiO_2 and Ag- doped TiO_2

TiO_2					
Number of neurons	Training MSE	Test MSE	Training R	Test R	All R
2	0.6711	0.2837	0.9968	0.9011	0.9958
4	0.8416	0.5812	0.996	0.9992	0.9945
6	1.1845	1.5597	0.9941	0.9569	0.9942
8	1.2987	1.2846	0.9939	0.8825	0.9861
10	1.4574	2.9371	0.9971	0.9988	0.9846
Ag-doped TiO_2					
2	0.8153	0.8675	0.9976	0.9994	0.9965
4	0.2900	0.6673	0.9986	1	0.9951
6	0.1460	0.2602	0.9993	0.9312	0.9966
8	0.3072	0.6144	0.9954	0.9996	0.9952
10	0.5092	0.7834	0.9989	0.9945	0.9921

The Fig. 9(a) and (b), show the ANN model with training, validation, test and overall R values for the copper with respect to TiO_2 and Ag-doped TiO_2. Similarly for the lead, it was shown in Fig. 10(a) and (b). The predicted R values for the copper and lead removal by TiO_2 and Ag-doped TiO_2 are found to be very good in training, validation, test and overall R values. These R values are close to + 1 which indicates a strong positive linear relationship with experimental data. For the copper Overall R with respect to Ag-doped TiO_2 is found to be 0.9968 and is better than that of TiO_2 value of 0.9958 showing a best fit for the experimental value. Similarly in lead the values found for the Ag-doped TiO_2 is 0.9966 showing better than that of TiO_2 value of 0.9958.

3.5 Comparison Between RSM and ANN Models

To check the reliability of models in a better way ANN and RSM predicted values are matched with the experimental values for the copper and lead with respect to TiO_2 and Ag-doped TiO_2, shown in Fig. 11(a) and (b) for copper and Fig. 12(a) and (b) for lead. The coefficient of determination (R^2)

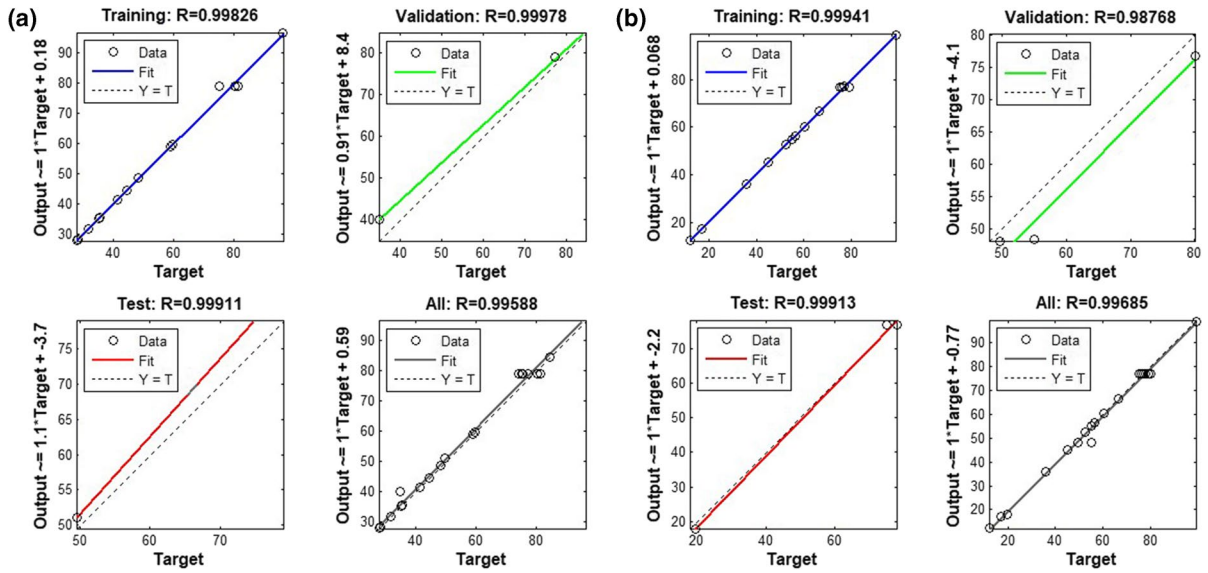

Fig. 9 **a** ANN model with training, test, validation and all prediction data set for copper removal by TiO_2. **b** ANN model with training, test, validation and all prediction data set for copper removal by Ag-doped TiO_2

for copper removal by TiO_2 and Ag-doped TiO_2 are found to be 0.8324 and 0.9177 respectively for the RSM (Fig. 7(a) and (b)) and with the ANN it is found to be 0.9918 and 0.9935 respectively (Fig. 11(a) and (b)).

The coefficient of determination (R^2) for lead removal by TiO_2 and Ag-doped TiO_2 found to be 0.9245 and 0.9403 respectively for the RSM (Fig. 8(a) and (b)) and with the ANN it is found to be 0.9915 and 0.9969 respectively (Fig. 12(a) and (b)). Our analysis

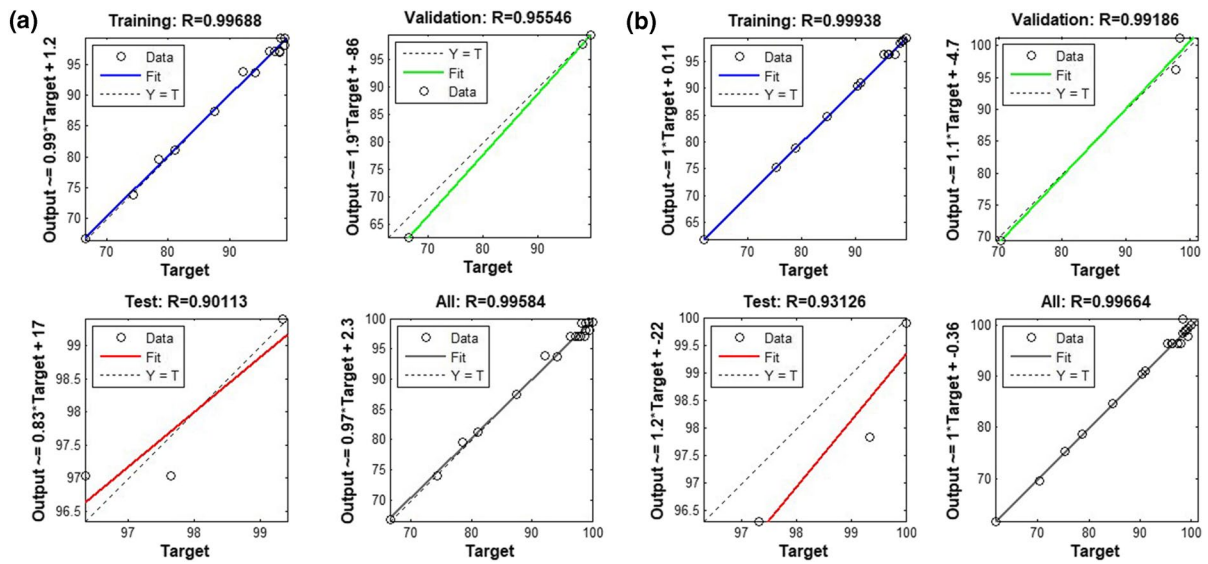

Fig. 10 **a** ANN model with training, test, validation and all prediction data set for lead removal by TiO_2. **b** ANN model with training, test, validation and all prediction data set for lead removal by Ag-doped TiO_2

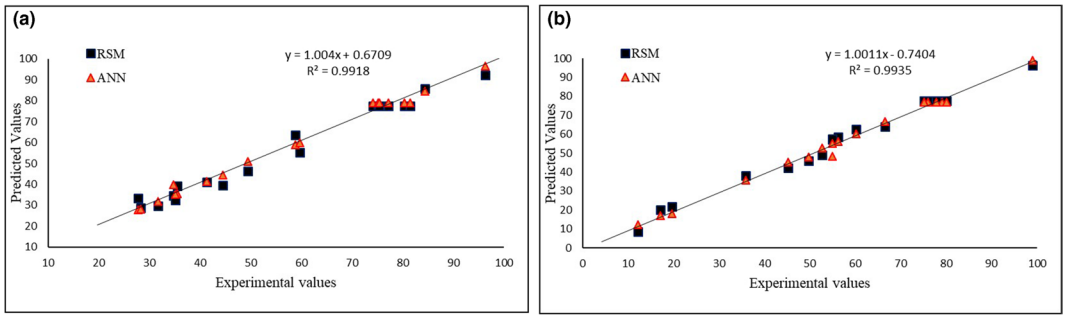

Fig. 11 **a** Comparison between experimental and predicted values of RSM and ANN for removal of copper from TiO_2. **b** Comparison between experimental and predicted values of RSM and ANN for removal of copper from Ag-doped TiO_2

indicates that the ANN models outperform the RSM models in predicting both copper and lead removal efficiencies with TiO_2 and Ag-doped TiO_2. The ANN predictions exhibit a closer fit to the experimental data, as evidenced by the smaller deviation from the ideal-fit line (experimental versus predicted) compared to RSM.

The RSM allows to consider the effects of relations on response differences and finally provides a quadratic mathematical equation that gives new predictions. The ANN gives process to simulate any form of nonlinearity (not only quadratic), thereby ANN is generally referred as a black box model, it employs analysis of existing data rather than designing a successful relationship. Therefore, the ANN offers a free hand and is not limited to the design of experiments in modelling.

For optimization in RSM, if we have good condition, the response is simply calculated from the found quadratic model. But we require the particular target to start the modeling process in ANN. Therefore, input (including variables and target value) must be added to the previous data. The difficulty is that the ANN has to predict the new target, which must be pre-inputted. Here, RSM can be successful as a strong predictor tool—completely solving the problem. In the first step, the values required for the ANN are provided by the values of CCD chart, and fed as preliminary estimation into ANN. In the second step, the complete input data is distributed into training, validation, and test subsections, and the reference data is allotted to the test subset. By ignoring the ANN test targets and creating them again, a fresh target is allotted to the target data. In this way, ANN can be used as a predictive model with RSM (Sabour & Amiri, 2017).

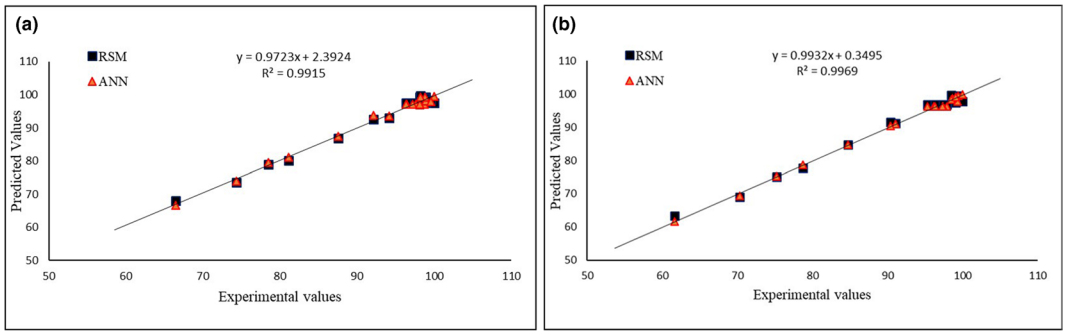

Fig. 12 **a** Comparison between experimental and predicted values of RSM and ANN for removal of lead from TiO_2. **b** Comparison between experimental and predicted values of RSM and ANN for removal of lead from Ag-doped TiO_2

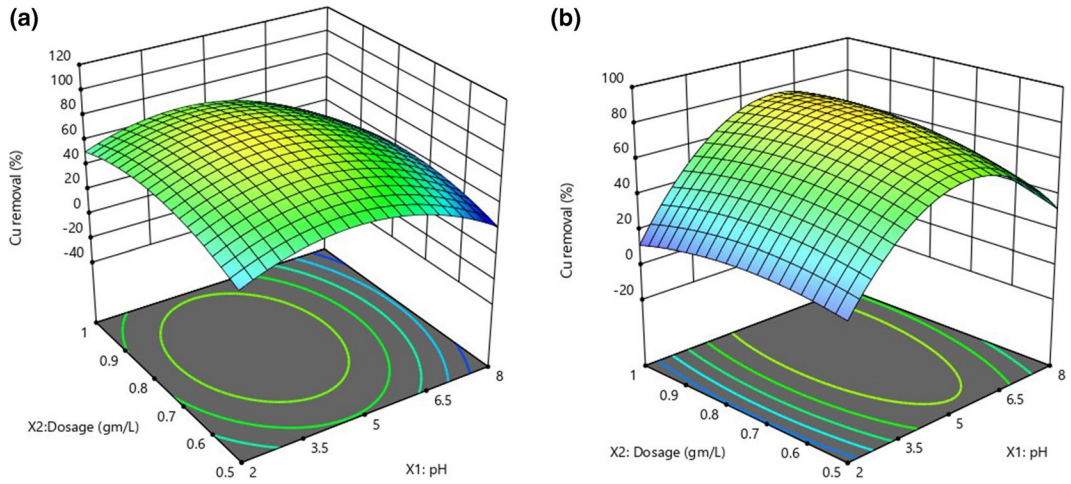

Fig. 13 **a** Three-dimensional surface graph pH and dosage effect on copper removal by TiO_2 (**b**) Three-dimensional surface graph pH and dosage effect on copper removal by Ag-doped TiO_2

3.6 Optimisation of pH, Dosage and Irradiation Time for the Copper Removal

3.6.1 Effect of pH on Removal of Copper and Lead from Synthetic Leachate

The removal of copper and lead from synthetic leachate is studied by three dimensional (3D) RSM graphs and contour plots. The three-dimensional graphs for copper and lead with respect to TiO_2 and Ag-doped TiO_2 are shown in Figs. 13 (a, b) and 14 (a, b). Similarly, Figs. 13 (c, d) and 14 (c, d) represents contour plots for copper and lead for the TiO_2 and Ag-doped TiO_2.

The Figs. 13 (a, b) and 14 (a, b) indicate the removal of copper and lead by TiO_2 and Ag-doped TiO_2 as a function of two variables pH and dosage, with irradiation time as constant of 100 min. The removal of copper is found to be 80.38% and 80.12% for TiO_2 and Ag-doped TiO_2 respectively at optimum pH of 5, dosage of 0.75 g/L at irradiation time of 100 min. The lead removal was found to be 97.2% and 96.34% for the TiO_2 and Ag-doped TiO_2 respectively for the same state.

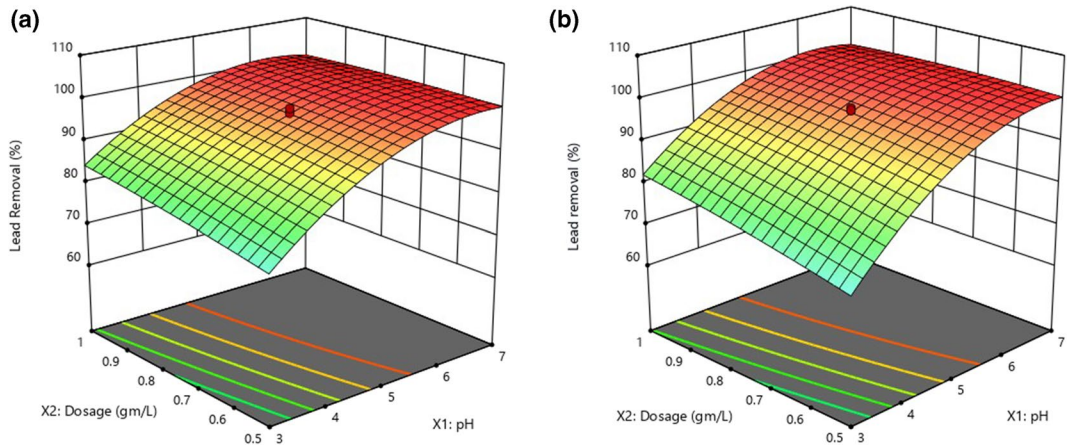

Fig. 14 **a** Three-dimensional surface graph pH and dosage effect on Lead removal by TiO_2 (**b**) Three-dimensional surface graph pH and dosage effect on lead removal by Ag-doped TiO_2

There is not much difference found in the removal of copper and lead for the Ag-doped TiO_2 compared to TiO_2. Zheng et al. (2015) studied the influence of silver on copper removal by photocatalysis and their results show that silver will decrease the copper reduction rate in photocatalysis because of redox potential of the Ag(I)/Ag(0) couple (0.799 V), which can compete more favourably with copper ions for electrons. The surface of the TiO_2 is amphoteric and it is essential to study the influence of pH on removal of copper and lead (Zheng et al., 2015).

From the Fig. 13(a) and (b) show the % removal as surface plots, from which it is observed that the maximum removal of copper is between pH 4 and 6.5. There is a reduction in copper removal percentage below pH 4 and above pH 6.5. When pH of solution is below 4 the adsorbent surface becomes more positive and removal of metal cations would be lowered (Kanakaraju et al., 2017). Other studies (Kanakaraju et al., 2017; Wahyuni et al., 2015) show that copper removal is maximum at neutral and alkaline states because of precipitation of metal on the surface of the nanomaterial. But in the present study percentage of copper reduction is observed to be minimum in neutral and alkaline stages, which may be due to the addition of EDTA as a hole scavenger (Yang & Lee, 2005). At a pH 7 and above, most of copper and EDTA exist in liquid phase due to the behaviour of ligand-type adsorption.

From the Fig. 14(a) and (b) it is observed that, the lead removal efficiency is found to be less in acidic condition compared to neutral and alkaline state for both the TiO_2 and Ag-doped TiO_2. In the present study at a pH of 3 the lead removal is found to be 78.53% and 75.23% for the TiO_2 and Ag-doped TiO_2 respectively at a dosage of 0.5 g/L with irradiation time of 150 min. Similarly, at a pH of 2 the lead removal efficiency is found to be 66.49% and 61.67% for the TiO_2 and Ag-doped TiO_2 respectively at a dosage of 0.75 g/L with irradiation time of 100 min. In Acidic conditions both Pb^{2+} and TiO_2 have attained a positive charge and there would be electrostatic repulsion between them which slows down the interface within OH^-/O^{2-} with Pb(II) to form Pb oxide/hydroxide complexes (Sreekantan et al., 2014) which in turn reduces the lead removal efficiency from the synthetic leachate.

The lead content in the solution with pH 1 to 8, is found as Pb^{2+} only, which can be oxidized by OH radicals from water and photocatalyst. The lead removal at pH 5 has been found to be 97.2% and 96.34% for the TiO_2 and Ag-doped TiO_2 respectively with dosage of 0.75 g/L and irradiation time of 100 min respectively. Similarly, at a pH of 7 the lead removal is found to be 98.2% and 98.45% for the TiO_2 and Ag-doped TiO_2 respectively with a dosage of 0.5 g/L and irradiation time of 150 min. The TiOH will be formed on the surface of TiO_2 at pH 5 to 8, which will provide more electrons for photocatalysis, leading to the higher degree of photo reduction. It should be noted that TiOH releases electrons and OH radicals easily. In the present study the lead removal is found to be 100% at pH 8 for the TiO_2 and Ag-doped TiO_2 with a dosage of 0.75 g/L and irradiation time of 100 min. At a pH 8 or above, lead will be in the form of $Pb(OH)_2$ which precipitate in water or stacked on the surface of TiO_2, which goes undetected by Atomic Absorption Spectroscopy (AAS) (Wahyuni et al., 2015). The results of removal of copper in the present study are in line with the study conducted by Yeber et al. (2009) (Yeber et al., 2009).

3.6.2 *Effect of Dosage on Removal of Copper and Lead from Synthetic Leachate*

The effect of dosage of TiO_2 and Ag-doped TiO_2 on removal of copper and lead is shown in Figs. 15 and 16 as a function of dosage and irradiation time. It is observed that as the dosage increases the removal percentage of copper and lead also increases. Increase in dosage of catalyst in the leachate help to increase of active sites of catalyst for the adsorption of metal ions from the synthetic leachate. Further the Cu (II) will reduce to Cu (I) in the presence of EDTA by the formation of electron hole pairs on the surface of semiconductor and increased hydroxyl radicals (Kabra et al., 2008).

From Figs. 15(a, b) and 16(a, b) it is observed that, above 0.75 g/L, there is a decrease in the percentage removal of copper and lead. This is due to excessive dosage above the saturation level can reduce the light adsorption coefficient or penetration due to the shielding effect (Julkapli & Bagheri, 2018). Furthermore, increasing the dosage can lead agglomeration of particulates, which reduces the active sites on the semiconductor surface (Alalm et al., 2014; Desai & Soraganvi, 2019).

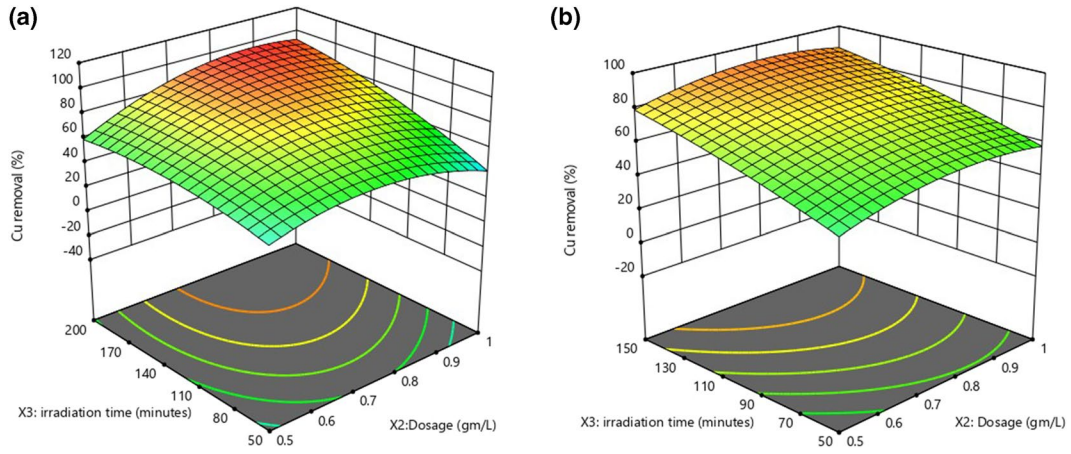

Fig. 15 **a** Three-dimensional surface graph dosage and irradiation time effect on copper removal by TiO_2 (**b**) Three-dimensional surface dosage and irradiation time effect on copper removal by Ag-doped TiO_2

3.6.3 Effect of Irradiation Time on Removal of Copper and Lead from Synthetic Leachate

The effect of irradiation time toward copper and lead removal by TiO_2 and Ag-doped TiO_2 is shown in Figs. 17 and 18 as function of pH and irradiation time. From the Figs. 17(a, b) and 18(a, b) the removal of copper and lead will increase with the increased irradiation time. For the irradiation time interval considered in the graph, there is no decrease in the irradiation time curve for removal of copper and lead as seen in the dosage effects. This increase of irradiation time in photocatalysis process helps in generating of more $OH^{\bullet}$ radicals, speeding up mixing and dispersion of adsorbent into the solution which helps in removal of copper and lead from synthetic leachate (Sahar et al., 2018) with respect to time. Kumar and Pandey (2017) reported reaction rate reduces with irradiation time as it follows the pseudo first-order kinetics. The high irradiation time will decrease the removal efficiency of lead and copper from synthetic leachate. This may be due to the occurrence of end of the reaction where less number of free radicals will generate and affects the lead removal efficiency. Therefore, optimum irradiation time for copper and lead removal from the synthetic leachate is found to be 100 min for the present study.

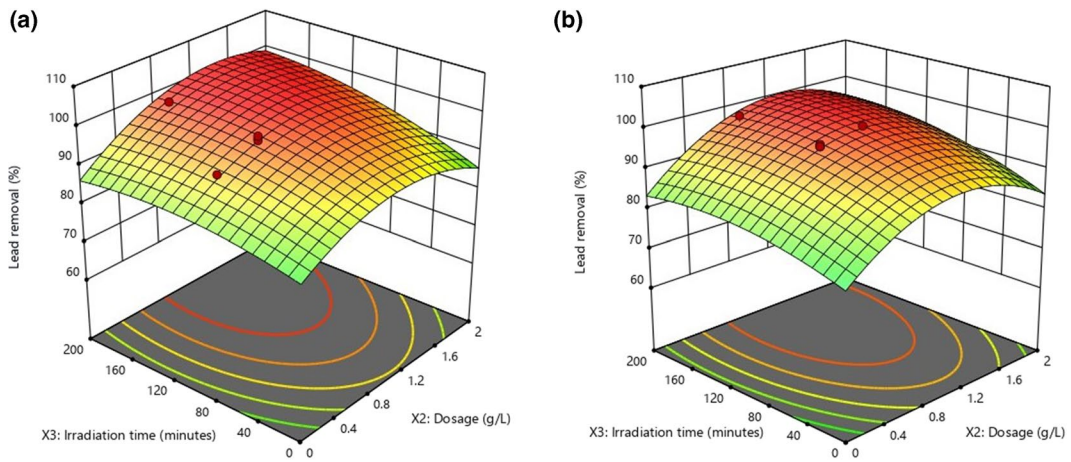

Fig. 16 **a** Three-dimensional surface graph dosage and irradiation time effect on lead removal by TiO_2 (**b**) Three-dimensional surface dosage and irradiation time effect on lead removal by Ag-doped TiO_2

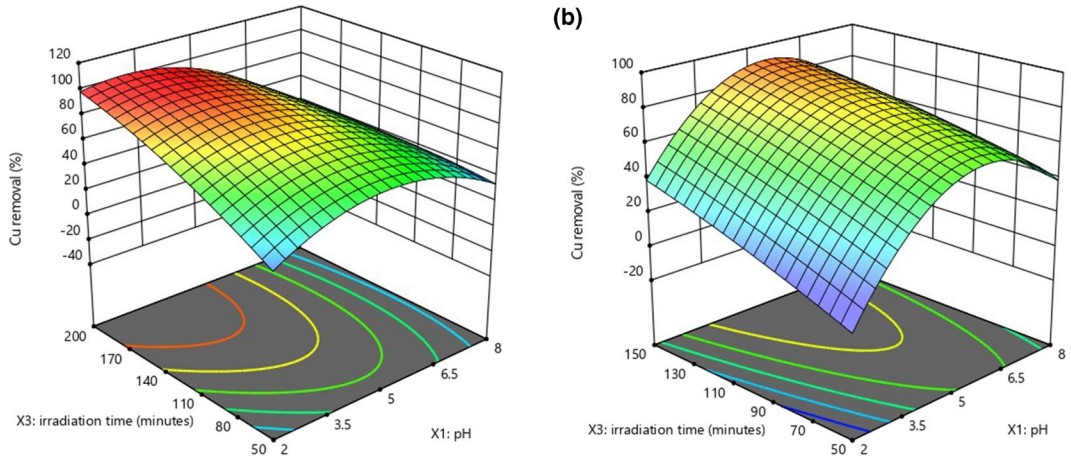

Fig. 17 **a** Three-dimensional surface graph pH and irradiation time effect on copper removal by TiO_2 (**b**) Three-dimensional surface pH and irradiation time effect on copper removal by Ag-doped TiO_2

Several studies have investigated the effect of irradiation time on the removal of heavy metals using various photocatalysts. While the optimal irradiation time can vary depending on the specific experimental conditions, our finding of 100 min aligns well with the trends observed in the literature. Kanakaraju et al. (2017) investigated copper removal from aquesous solution using TiO_2/ZnO-CaAlg photocatalyst and reported that 120 min were required for the removal of 87% of copper removal. Another study by Peter et al. (2012) focused on the removal of copper and lead from aqueous solution and found that the best removal efficiency was achieved after 60 min of irradiation time using a nano structured TiO_2/zeolite system based photocatalyst. Considering these findings and other relevant literature, our result of 100 min as the optimum irradiation time falls within the range of typical values reported in previous studies. This consistency further supports the reliability of our experimental results and validates the effectiveness of our photocatalytic system in removing copper and lead from synthetic leachate.

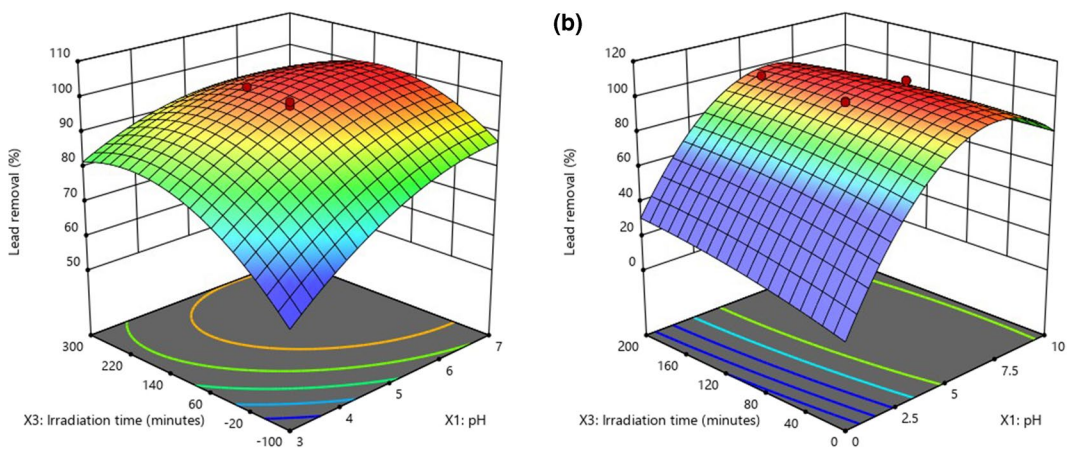

Fig. 18 **a** Three-dimensional surface graph pH and irradiation time effect on lead removal by TiO_2 (**b**) Three-dimensional surface pH and irradiation time effect on lead removal by Ag-doped TiO_2

3.6.4 Mechanism of Copper and Lead Removal using TiO2

The basic reactions are expressed for removal of Cu (II) by TiO_2 in photocatalysis is expressed as follows in Eqs. 11 to 14. (Litter, 2009; Murruni et al., 2007)

$$2[(Ti0_2) + h\nu \rightarrow e^- + h^+] \quad (11)$$

$$Cu^{2+} + 2e^- \rightarrow Cu \quad (12)$$

$$H_2O + 2h^+ \rightarrow {}^1/_{2O_2} + 2H^+ \quad (13)$$

$$Cu^{2+} + H_2O + h\nu \rightarrow Cu + {}^1/_{2O_2} + 2H^+ \quad (14)$$

Complete reduction of Cu(II) was observed in UV illuminated TiO_2 suspensions containing methanol, although, no reduction was possible in the absence of methanol (Kabra et al., 2008). In the present study EDTA is used as hole scavenger and Foster et al. (1993) reported that Cu(II) could be reduced to Cu(I) in the presence of suitable organics only, such as sodium formate and EDTA, and complete reduction was not observed. The present results of the study show removal of copper is 80.38% and 80.12% for TiO_2 and Ag-doped TiO_2 respectively at optimum pH of 5, dosage of 0.75 g/L at an irradiation time of 100 min.

The Pb(II) metal ions treated by TiO_2, photocatalytic reduction meet thermodynamic requirements, the general procedure is followed by successive one-electron cutting steps until the final stable species is formed. The general pathway for Pb(II) reduction to metallic lead is as follows in Eqs. 15 and 16. (Litter, 2009; Murruni et al., 2007)

$$Pb^{2+} + e^- \rightarrow Pb^+ \quad (15)$$

$$Pb^+ + e^- \rightarrow Pb(0) \quad (16)$$

The anodic reaction would be the oxidation of water by holes and ending in protons and oxygen as show in Eq. 17

$$H_2O + h^+ \rightarrow\rightarrow\rightarrow {}^1/_{2O_2} + 2H^+ \quad (17)$$

The oxidative route to Pb (IV) species through hole or $OH^\bullet$ attack is one possible process. The global reaction is as in Eq. 18

$$2Pb^{2+} + 2H_2O + O_2 \rightarrow 2PbO_2 + 4H^+ \quad (18)$$

In this route, PbO_2 is formed as the final product, obtained as a dark brown deposit on TiO_2. Considering two consecutive one-electron charge-transfer steps, the first one will be h^+_{vb} or $OH^\bullet$ attack leading to the trivalent state as shown in Eq. 19. (Litter, 2009; Murruni et al., 2007)

$$h^+_{Vb}/H^\bullet + Pb(II) \rightarrow Pb(III) \quad (19)$$

3.7 Kinetic Study for the Removal of Copper and Lead by TiO_2 and Ag-doped TiO_2

The photocatalytic reaction rate of metals is expressed by the pseudo-first-order kinetic model, because reduction pattern of metals is better in first order compared to zero and second order equations.

The suitability of the L–H model is verified for the removal of copper and lead with coefficient of determination (R^2) as shown in Figs. 19 and 20 for TiO_2 and Ag-doped TiO_2. The R^2 obtained for removal of copper by TiO_2 and Ag-doped TiO_2 found to be 0.8821 and 0.8681 respectively by Fig. 19(a) and (b). Similarly for removal of lead by TiO_2 and Ag-doped TiO_2 found to be 0.8228 and 0.8341 respectively by Fig. 20(a) and (b). The higher values of R^2 in both the cases confirms that the photocatalytic removal of copper and lead using TiO_2 and Ag-doped TiO_2 obey pseudo-first order kinetics. The slope of apparent reaction rate constant (K_{app}) is calculated for the removal of copper and lead by plotting $ln = (\frac{C}{C_0})$ vs time. The K_{app} for removal copper by TiO_2 and Ag-doped TiO_2 found to be 1.56×10^{-2} min^{-1} and 1.405×10^{-2} min^{-1} respectively. Similarly for the removal of lead, K_{app} found to be 2.1×10^{-2} min^{-1} and 2.05×10^{-2} min^{-1} by TiO_2 and Ag-doped TiO_2 respectively. From the K_{app} result it is observed that Ag-doped TiO_2 rate constant is smaller than that of TiO_2. Zheng et al. (2015) (Zheng et al., 2015) studied the effect of silver on copper reduction from kinetic analysis and found that the rate of copper reduction steadily declined during the

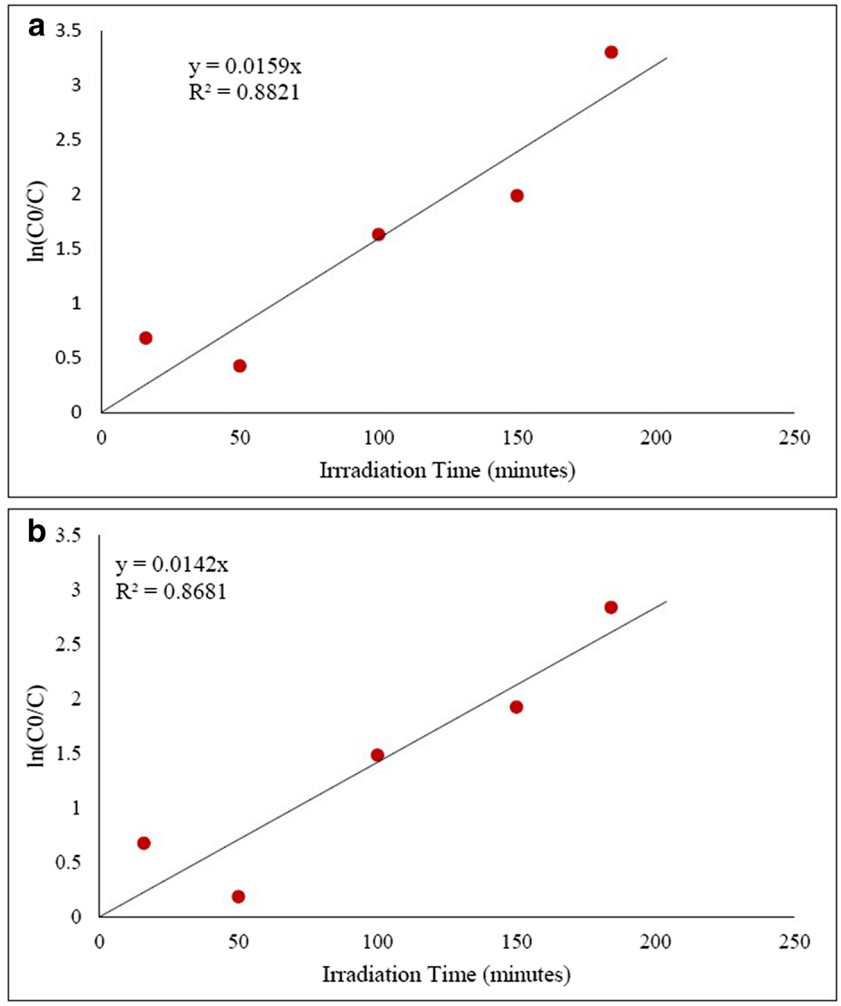

Fig. 19 **a** Kinetic plot of $ln = (\frac{C}{C_0})$ vs time for removal of copper by TiO_2. **b** Kinetic plot of $ln = (\frac{C}{C_0})$ vs time for removal of copper by Ag-doped TiO_2

first $\left(3.44 \times 10^{-2} to 9.30 \times 10^{-3} min^{-}\right)$ and second $\left(7.65 \times 10^{-3} to 1.50 \times 10^{-3} min^{-}\right)$ regime. This is because of Ag (0) is formed after Ag (I) photo reduction and the formed Ag (0) species are present on the surface of TiO_2, which reduces the photo-catalytic activity of TiO_2.

3.8 Recycling of TiO_2 and Ag-doped TiO_2 Nanomaterials

The toxicity of doped or undoped nanoparticles is related to their small size, ability to produce reactive oxygen species and large surface area (Taghavi et al., 2013). Many researchers have studied the reuse and recovery of catalyst in the photocatalysis, which can help reduce the nanomaterial effects in the environmental and the operational costs in treatment of wastewater/leachate. Some studies have shown the reuse of TiO_2 and doped TiO_2 in the removal of organic, inorganic and heavy metals. Cheng et al. (2019) show that, Cu(II) removal efficiency decreased from 96.8% to 89.6% after using four cycles of TiO_2/titanate nanotube composite (TiNT), that is quite acceptable. The photocatalytic activity of TiO_2/TiNTs is mainly contributed by TiO_2, which is more stable during the application and regeneration process. The TiO_2/TiNTs also has good settling performance, which facilitates its separation from aqueous solution after application. Ismail et al. (2008) investigated the Sorption of $Ni^{2+}$and Cd^{2+} by the binary oxide TiO_2-SiO_2. The Cd^{2+} was removed at 100% after using 10 cycles, while the Ni^{2+} sorption

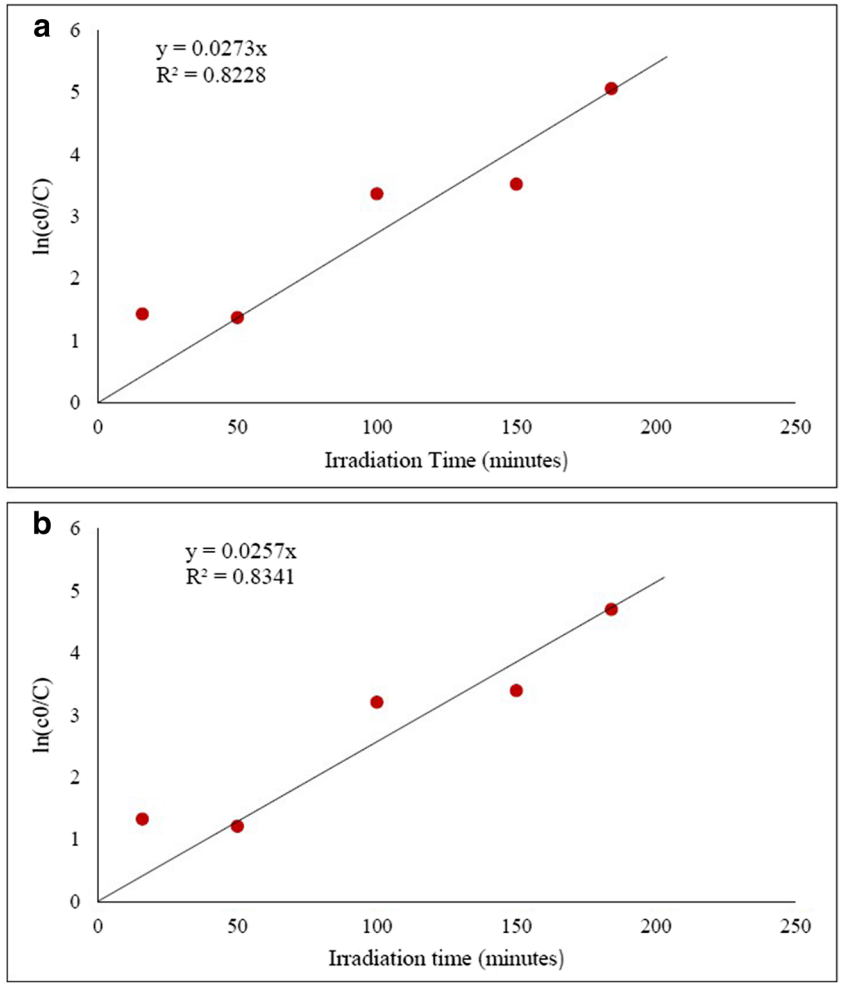

Fig. 20 **a** Kinetic plot of $ln = (\frac{C}{C_0})$ vs time for removal of lead by TiO_2. **b** Kinetic plot of $ln = (\frac{C}{C_0})$ vs time for removal of lead by Ag-doped TiO_2

decreased sharply after 6 cycles by TiO_2-SiO_2. This is apparently because Cd^{2+} has a higher affinity to form hydroxyl complexes than does Ni^{2+}(Ismail et al., 2008). Djellabi and Ghorab, (2015) show, Cr(VI) reduction rate decreased from 89% to 67.1% in the fifth use of TiO_2-immobilized. This decrease of the removal rate can be accounted for the saturation of photocatalyst surface by the Cr(III) ions deposited during the reduction reaction. With these studies we can conclude used nanomaterials can be regenerated and reused, but the efficiency of metal removal will be reduced.

The widespread use of TiO_2 and Ag doped TiO_2 nanomaterials in the field of environmental protection, agriculture and medicine has increased the release of these materials in the environment. These nanomaterials enter the human body through the skin, intestines and lungs and affect various organs of the body (Malakar et al., 2020). Regular supply of small amount of TiO_2 affects the intestinal mucosa, heart, brain and other internal organs of the human body (Baranowska-Wójcik et al., 2020). Only when these TiO_2 reaches adequate levels in the natural environment, they can pose a significant risk to environmental biota (Mo et al., 2016). Ag-doped TiO_2 nanomaterials are more toxic than TiO_2, because TiO_2 doped with silver oxide or silver carbonate reduces the size of TiO_2 nanomaterials and have synergistic effects on adult zebrafish at the molecular and cellular levels (Mahjoubian et al., 2021). Ag-doped TiO_2 nanomaterials induce toxicity in human liver cancer (HepG2) cells via oxidative stress (Ahamed et al., 2017). But it has also been debated that, Titanium dioxide (TiO_2) is a natural oxide of the element titanium with low toxicity, and negligible biological effects (Grande & Tucci, 2016).

Table 9 Summary of performance of TiO_2 and structurally modified TiO_2 in removal of copper from wastewater/aqueous solution

Sl No	Wastewater type	TiO_2	pH	Dosage in (g/L)	Irradiation time in (Hours)	Light details	Hole scavengers	% of copper removal	Reference
1	Aqueous solution	Degussa P-25 TiO_2	4.3	0.5	1 h 10 min	120 W UV-C lamp (254 nm)	Nil	80%	(Yeber et al., 2009)
2	N, N'-ethylenediamine-disuccinic acid (EDDS) and Cu (II) ions	TiO_2 Nanomaterial	2	0.05	1	125 W Hg vapour lamp (λ = 300–400 nm) & Natural Sunlight	Nil	85%	(Satyro & Carroll 2014)
3	Aqueous solution	TiO_2 powder	5	0.05	24	40 W UV (λ = 290-390 nm)	Nil	45.56%	(Wahyuni et al., 2015)
4	Synthetic wastewater	TiO_2 (Merck)	8	1	8	Parabolic collector -Sunlight	Citric acid	97.6%	(Kabra et al., 2008)
5	Synthetic (CU^{2+} (II):CN)	Degussa P-25 TiO_2	11	1	3.5	100 W high-pressure mercury lamp (λ = 228–420 nm)	–	90%	(Barakat et al. 2004)
6	Aqueous solution	TiO_2@yeast	5	0.75	1	UV-light lamp	–	70.2%	(Zheng et al., 2015)
7	Aqueous solution	nano-structured TiO_2 / zeolite system	4	101 g/L	1	Solar light with magnetic stirrer 160 rpm	Nil	46.3%	(Peter et al., 2012)
8	Aqueous solution	TiO_2/ZnO–CaAlg	5	1 gm	2	ultraviolet (UV) lamp (λ = 254 nm)	–	87%	(Kanakaraju et al., 2017)
9	Cu(II) Aqueous solution	TiO_2	3	1.0	0.5	125W high pressure mercury lamp (λ = 546)	Formic acid	60%	(Aman et al., 2011)
10	Cu(II) Aqueous solution	TiSi	3	1.0	0.5	125W high pressure mercury lamp (λ = 546)	Formic acid	38%	(Aman et al., 2011)
11	Cu(II) Aqueous solution	TiZr	3	1.0	0.5	125W high pressure mercury lamp (λ = 546)	Formic acid	70%	(Aman et al., 2011)
12	Cu(II) Aqueous solution	TiO_2	3	1.0	0.5	125W high pressure mercury lamp (λ = 546)	EDTA	62%	(Aman et al., 2011)
13	Cu(II) Aqueous solution	TiSi	3	1.0	0.5	125W high pressure mercury lamp (λ = 546)	EDTA	42%	(Aman et al., 2011)
14	Cu(II) Aqueous solution	TiZr	3	1.0	0.5	125W high pressure mercury lamp (λ = 546)	EDTA	80%	(Aman et al., 2011)
15	Synthetic Leachate	Sisco Research TiO_2	5	0.75	1 h 40 min	Natural sunlight	EDTA	80.38%	Present study
16	Synthetic Leachate	Ag-doped TiO_2	5	0.75	1 h 40 min	Natural sunlight	EDTA	80.12%	Present study

Table 10 Summary of performance of TiO_2 and structurally modified TiO_2 in removal of lead from wastewater/aqueous solution

Sl No	Wastewater type	TiO_2	pH	Dosage in (g/L)	Irradiation time in (Hours)	Light details	Hole scavengers	% of lead Removal	Reference
1	Aqueous solution	TiSi of 10%	3.5	1.5	1	125 W UV lamp	Sodium formate	96%	(Mishra et al., 2007)
2	Aqueous solution	TiZr of 10%	3.5	1.5	1	Visible light	Sodium formate	93%	(Mishra et al., 2007)
3	Aqueous solution	Degussa P-25 TiO_2	3	1	5	UV lamp (15 W)	Ozone	35%	(Murruni et al., 2007)
4	Aqueous solution	Pt–TiO_2	3	1	5	UV lamp (15 W)	Oxygen	93%	(Murruni et al., 2007)
5	Aqueous solution	Pt–TiO_2	3	1	5	UV lamp (15 W)	ozone	83%	(Murruni et al., 2007)
6	Synthetic wastewater	TiO_2 (Merck)	8	2	8	Parabolic collector -Sunlight	Citric acid	46%	(Kabra et al., 2008)
7	Aqueous solution	TiO_2 powder	5	0.05	24	40 W UV (λ = 290-390 nm)	Nil	40.32%	(Wahyuni et al., 2015)
8	Aqueous solution	nano-structured TiO_2 / zeolite system	4	101 g/L	1	Solar light with magnetic stirrer 160 rpm	Nil	41.8%	(Peter et al., 2012)
9	Synthetic Leachate	Sisco Research TiO_2	5	0.75	1 h 40 min	Natural sunlight	Acetic acid	97.2%	Present study
10	Synthetic Leachate	Ag-doped TiO_2	5	0.75	1 h 40 min	Natural sunlight	EDTA	96.34%	Present study

3.9 Comparative Study Between Present Study and Other Studies

Tables 9 and 10 show a summary of copper and lead removal of TiO_2 and structurally modified TiO_2 with respect to pH, dosage, irradiation time and hole scavenger. The removal of more than 70% of copper from synthetic wastewater and aqueous solution is observed with TiO_2 and structurally modified TiO_2. The reason for excessive removal of copper from aqueous solution/wastewater may be due to high intensity of light and hole scavenger used in the treatment. Some studies shown in Table 9 show copper removal between 40 to 50%, where low-intensity of light/solar light is used and no hole scavengers are used for treatment. Copper and selenium removal as individual and mixed aqueous solutions were studied simultaneously by Aman et al. (2011) using TiO_2 and structurally modified TiO_2 under visible light conditions. The formic acid and EDTA are used as hole scavengers for the treatment. EDTA acts as a better hole scavenger than formic acid for copper reduction. The enhanced photocatalytic reduction in the presence of EDTA may be due to the strong adsorption of the metal-EDTA complex on the catalytic surface.

The literature presented in Table 10 highlights lead removal from aqueous solution using hole scavengers such as oxygen, ozone and sodium sulphate with structurally modified TiO_2. The low percentage of lead reduction at pH 8, 5 and 4 may be attributed to low light intensity and solar radiation used at this pH.

The present study shows removal of copper from the synthetic leachate as 80.38% and 80.12% for TiO_2 and Ag-doped TiO_2 respectively at optimum conditions of pH of 5, dosage of 0.75 g/L with irradiation time of 100 min. The lead removal efficiency is found to be 97.2% and 96.34% for the TiO_2 and Ag-doped TiO_2 nanomaterials respectively, at an optimized pH of 5 and dosage of 0.75 g/L with irradiation time of 100 min. The constructed CPC is effective in capturing major photons from sunlight, resulting in higher copper and lead removal efficiency with shorter

contact time and lower catalyst dosage using natural sunlight, which is much better compared to other studies.

3.10 Scale Up and Cost Analysis for Photocatalysis

The total cost for photocatalysis includes sum of capital expenditures, operating expenses and maintenance. These costs are strongly dependent on the nature and concentration of leachate pollutants and photocatalysis stage adopted in the treatment unit. If photocatalysis is adopted at the primary and secondary stage of treatment unit, a large quantity of TiO_2 nanomaterial and increased photocatalysis timing will increase the cost of treatment for high concentration of leachate pollutants. Many researchers have suggested that photocatalysis is appropriate for treating pollutants in the final stage to meet the regulatory requirements. Where the cost of treatment will reduce.

Present research is performed at lab scale for treatment of 1L of leachate pollutants. The synthetic leachate was diluted for low metal concentrations to meet the requirement of final stage leachate characteristics. For performing lab scale study, the capital expenditure includes construction of compound parabolic collector and its accessories and it can be fabricated at a very low cost ($ 24) by providing the design. The operational cost includes TiO_2 nanomaterial as photocatalyst, EDTA and citric acid as hole scavengers. TiO_2 nanomaterial is comparatively expensive (25 gm is $ 73.55) and it is procured from the Sisco Research Laboratory. In literature production of TiO_2 using $TiCl_4$ is also presented, where in cost of TiO_2 nanomaterial can be brought down. The regeneration of the photocatalyst is another way to lower the cost where regeneration of catalyst can be done in a very simple way. Hole scavengers used in study are at very small quantity and their cost is negligibly less. The Maintenance cost includes washing of glass reactor and painting of compound parabolic collector with sliver for capturing maximum photons from sunlight.

Researchers have suggested Photocatalytic technology has been proven to be cost-effective alternative for treatment of wastewater containing persistent organic and inorganic pollutants (Jia et al., 2011; Wang, 2012) Compound parabolic photoreactors are best suited for near-term applications in pilot-scale (> 1000 L/day) because of their favourable light collecting characteristics and well-known design method.

4 Conclusions

The main aim of this study is to evaluate, the predictive capability of both ANN and RSM models in the removal of copper and lead from the synthetic leachate using TiO_2 and Ag-doped TiO_2 nanomaterials. The synthetic leachate prepared for the copper and lead shows the young leachate characteristics with high values of metal concentration and COD. The characterization study performed on the TiO_2 and Ag-doped TiO_2 nanomaterials confirms the used nanomaterials are in anatase phase having crystallite particle size 19.29 nm and 15.36 nm for TiO_2 and Ag-doped TiO_2 respectively. The shape of the nanomaterials by SEM is found to be spherical with dense agglomeration. The EDX results showed that 1% doping of Ag on TiO_2. The optimum conditions for copper and lead removal were found to be at a pH 5, the dosage of 0.75 gm/L with an irradiation time of 100 min. The quadratic models developed for copper and lead show that, experimental values obtained were in good agreement with the predicted values obtained by RSM. ANOVA showed a high determination of coefficient R^2 value greater than 0.80 for both copper and lead removal. The two statistical models ANN and RSM were compared to estimate photocatalysis performance in the removal of copper and lead from the synthetic leachate. The coefficient of determination (R^2) values of RSM and ANN for the copper and lead for TiO_2 and Ag-doped TiO_2 are found to be in good agreement. The ANN predicted values for copper and lead have less deviation with the experimental values compared to RSM. Therefore, ANN shows better performance in comparison to RSM in all aspects. The coefficient of determination R^2 values for copper and lead removal by TiO_2 and Ag-doped TiO_2 confirm, that the developed model allows the accurate prediction and we can use the RSM data as input to ANN for prediction. The kinetic study shows that, copper and lead removal by photocatalytic process are described well by the Langmuir–Hinshelwood kinetic model. In the present study Langmuir–Hinshelwood (L–H) model follows the pseudo-first-order rate constant. The Coefficient of determination R^2 values for copper and lead removal by TiO_2 and Ag-doped TiO_2 are found to be greater than 0.85 in kinetic model.

From the present study, it is observed that heavy metals such as lead and copper can be removed more than 90%, from the leachate using TiO_2 and Ag-doped

TiO_2 nanomaterials. Therefore, in tropical area, photocatalysis can be used as a final stage of treatment for complete removal of copper and lead from the leachate to meet the discharge standard limits regulated by the authority. The Method presented in this study can be scaled-up for the treatment of leachate economically by adopting reuse and recovery of the catalyst.

The problems encountered during the photocatalytic experiment for the removal of copper and lead using TiO_2 and Ag-doped TiO_2 are maintaining the desired pH level during experiments and another problem encountered is the precise quantification of copper and lead removal, which requires advanced analytical techniques.

Acknowledgements The Authors heartly thank all the staff members and research scholars of Civil and Mechanical Engineering departments for their support and help in this research work.

Data Availability The datasets generated during and/or analysed during the current study are available from the corresponding author on reasonable request.

Declarations

Conflict of Interest The authors declare no conflicts of interest.

References

Ahamed, M., Khan, M. A. M., Akhtar, M. J., Alhadlaq, H. A., & Alshamsan, A. (2017). Ag-doping regulates the cytotoxicity of TiO_2 nanoparticles via oxidative stress in human cancer cells. *Scientific Reports, 7*(1), 1–14. https://doi.org/10.1038/s41598-017-17559-9

Alalm, M. G., Tawfik, A., & Chemicals, A. (2014). Solar photocatalytic degradation of phenol in aqueous solutions using titanium dioxide. *International Journal of Chemical, Molecular, Nuclear, Materials and Metallurgical Engineering, 8*(2), 136–139.

Ali, I. H., Siddeeg, S. M., Idris, A. M., Brima, E. I., Ibrahim, K. A., Ebraheem, S. A. M., & Arshad, M. (2021). Contamination and human health risk assessment of heavy metals in soil of a municipal solid waste dumpsite in Khamees-Mushait, Saudi Arabia. *Toxin Reviews, 40*(1), 102–115. https://doi.org/10.1080/15569543.2018.1564144

Aman, N., Mishra, T., Hait, J., & Jana, R. K. (2011). Simultaneous photoreductive removal of copper (II) and selenium (IV) under visible light over spherical binary oxide photocatalyst. *Journal of Hazardous Materials, 186*(1), 360–366. https://doi.org/10.1016/j.jhazmat.2010.11.001

APHA. (1999). Standard methods for the examination of water and wastewater / prepared and published jointly by the American Public Health Association, American Water Works Association, Water Pollution Control Federation ; joint editorial board, Michael J. Taras, Arnold, 2671.

Bandala, E. R., Liu, A., Wijesiri, B., Zeidman, A. B., & Goonetilleke, A. (2021). Emerging materials and technologies for landfill leachate treatment: A critical review. *Environmental Pollution, 291*(September), 118133. https://doi.org/10.1016/j.envpol.2021.118133

Barakat, M. A., Chen, Y. T., & Huang, C. P. (2004). Removal of toxic cyanide and Cu (II) Ions from water by illuminated TiO2 catalyst. *Applied Catalysis B: Environmental, 53*(1), 13–20.

Baranowska-Wójcik, E., Szwajgier, D., Oleszczuk, P., & Winiarska-Mieczan, A. (2020). Effects of titanium dioxide nanoparticles exposure on human health—a review. *Biological Trace Element Research, 193*(1), 118–129. https://doi.org/10.1007/s12011-019-01706-6

Batool, F., Akbar, J., Iqbal, S., Noreen, S., Nasir, S., & Bukhari, A. (2018). Study of isothermal, kinetic, and thermodynamic parameters for adsorption of cadmium: An overview of linear and nonlinear approach and error analysis. *Bioinorganic Chemistry and Applications, 2018*, 1–11. https://doi.org/10.1155/2018/3463724

Boateng, T. K., Opoku, F., & Akoto, O. (2019). Heavy metal contamination assessment of groundwater quality: A case study of Oti landfill site, Kumasi. *Applied Water Science, 9*(2), 1–15. https://doi.org/10.1007/s13201-019-0915-y

Champagne, P., & Li, C. (2009). Use of Sphagnum peat moss and crushed mollusk shells in fixed-bed columns for the treatment of synthetic landfill leachate. *Journal of Material Cycles and Waste Management, 11*(4), 339–347. https://doi.org/10.1007/s10163-009-0262-4

Cheng, K., Cai, Z., Fu, J., Sun, X., Sun, W., Chen, L., et al. (2019). Synergistic adsorption of Cu(II) and photocatalytic degradation of phenanthrene by a jaboticaba-like TiO2/titanate nanotube composite: An experimental and theoretical study. *Chemical Engineering Journal, 358*(Ii), 1155–1165. https://doi.org/10.1016/j.cej.2018.10.114

Desai, N. N., & Soraganvi, V. S. (2019). Performance of TiO_2 photocatalytic nanomaterial in removal of lead from sanitary landfill leachate using sunlight. *Waste Valorisation and Recycling* (pp. 467–476). Springer Nature Singapore. https://doi.org/10.1007/978-981-13-2784-1

Djellabi, R., & Ghorab, M. F. (2015). Photoreduction of toxic chromium using TiO_2-immobilized under natural sunlight: Effects of some hole scavengers and process parameters. *Desalination and Water Treatment, 55*(7), 1900–1907. https://doi.org/10.1080/19443994.2014.927335

Foster, N. S., Noble, R. D., & Koval, C. A. (1993). Reversible photoreductive deposition and oxidative dissolution of copper ions in titanium dioxide aqueous suspensions. *Environmental Science and Technology, 27*(2), 350–356. https://doi.org/10.1021/es00039a016

Gomes, J., Lopes, A., Bednarczyk, K., Gmurek, M., Stelmachowski, M., Zaleska-Medynska, A., et al. (2018). Effect of noble metals (Ag, Pd, Pt) loading over the efficiency of TiO_2 during photocatalytic ozonation on the toxicity of parabens. *ChemEngineering, 2*(1), 4. https://doi.org/10.3390/chemengineering2010004

Gopinath, K. P., Madhav, N. V., Krishnan, A., Malolan, R., & Rangarajan, G. (2020). Present applications of titanium dioxide for the photocatalytic removal of pollutants from water: A review. *Journal of Environmental Management, 270*(March), 110906. https://doi.org/10.1016/j.jenvman.2020.110906

Grande, F., & Tucci, P. (2016). Titanium dioxide nanoparticles: A risk for human health? *Mini-Reviews in Medicinal Chemistry, 16*(9), 762–9. https://doi.org/10.2174/1389557516666160321114341

Haykin, S. (2014). *Neural networks and learning machines* (3rd edition). Pearson.

Herrmann, H., & Bucksch, H. (2014). Standard condition. *Dictionary geotechnical engineering/Wörterbuch GeoTechnik* (pp. 1–122). https://doi.org/10.1007/978-3-642-41714-6_196623

Hussein, M., Yoneda, K., Mohd-Zaki, Z., Amir, A., & Othman, N. (2021). Heavy metals in leachate, impacted soils and natural soils of different landfills in Malaysia: An alarming threat. *Chemosphere, 267*, 128874. https://doi.org/10.1016/j.chemosphere.2020.128874

Ilyas, H., Qazi, I. A., Asgar, W., Awan, M. A., & Khan, Z. U. D. (2011). Photocatalytic degradation of nitro and chlorophenols using doped and undoped titanium dioxide nanoparticles. *Journal of Nanomaterials*, *2011*. https://doi.org/10.1155/2011/589185

Ismail, A. A., El-Midany, A. A., Ibrahim, I. A., & Matsunaga, H. (2008). Heavy metal removal using SiO_2-TiO_2 binary oxide: Experimental design approach. *Adsorption, 14*(1), 21–29. https://doi.org/10.1007/s10450-007-9042-4

Jia, C., Wang, Y., Zhang, C., & Qin, Q. (2011). UV-TiO_2 photocatalytic degradation of landfill leachate. *Water, Air, & Soil Pollution, 217*(1–4), 375–385. https://doi.org/10.1007/s11270-010-0594-7

Jin, L., Nikiforuk, P. N., & Gupta, M. M. (2002). Neural networks for modelling and control of discrete-time nonlinear systems. 1122–1127. https://doi.org/10.1109/icsmc.1994.399994

Julkapli, N. M., & Bagheri, S. (2018). Applications of Titania as a heterogeneous. *Nanocatalysts in environmental applications* (pp. 51–67). https://doi.org/10.1007/978-3-319-69557-0_4

Kabra, K., Chaudhary, R., & Sawhney, R. L. (2008). Solar photocatalytic removal of Cu(II), Ni(II), Zn(II) and Pb(II): Speciation modeling of metal-citric acid complexes. *Journal of Hazardous Materials, 155*(3), 424–432. https://doi.org/10.1016/j.jhazmat.2007.11.083

Kanakaraju, D., Ravichandar, S., & Lim, Y. C. (2017). Combined effects of adsorption and photocatalysis by hybrid TiO2/ZnO-calcium alginate beads for the removal of copper. *Journal of Environmental Sciences (china), 55*, 214–223. https://doi.org/10.1016/j.jes.2016.05.043

Kanmani, S., & Gandhimathi, R. (2013). Assessment of heavy metal contamination in soil due to leachate migration from an open dumping site. *Applied water science, 3*, 193–205.

Kulkarni, R. M., Malladi, R. S., Hanagadakar, M. S., Doddamani, M. R., & Bhat, U. K. (2016). Ag-TiO2 nanoparticles for photocatalytic degradation of lomefloxacin. *Desalination and Water Treatment, 57*(34), 16111–16118. https://doi.org/10.1080/19443994.2015.1076352

Kumar, A., & Pandey, G. (2017). A review on the factors affecting the photocatalytic degradation of hazardous materials. *Material Science & Engineering International Journal, 1*(3), 106–114. https://doi.org/10.15406/mseij.2017.01.00018

Li, Y. M., Wang, Y., Chen, M. J., Huang, T. Y., Yang, F. H., & Wang, Z. J. (2023). Current status and technological progress in lead recovery from electronic waste. *International Journal of Environmental Science and Technology, 20*(1), 1037–1052.

Lin, L., Jiang, W., Chen, L., Xu, P., & Wang, H. (2020). Treatment of produced water with photocatalysis: Recent advances, affecting factors and future research prospects. *Catalysts*, *10*(8). https://doi.org/10.3390/catal10080924

Litter, M. I. (2009). *Chapter 2 - Treatment of chromium, mercury, lead, uranium, and arsenic in water by heterogeneous photocatalysis*. *Advances in chemical engineering* (First Edit., Vol. 36). Elsevier. https://doi.org/10.1016/S0065-2377(09)00402-5

Litter, M. I. (2015). Mechanisms of removal of heavy metals and arsenic from water by TiO_2 -heterogeneous photocatalysis, Conference paper. *Pure and Applied Chemistry, 2015*. https://doi.org/10.1515/pac-2014-0710

Mahjoubian, M., Naeemi, A. S., & Sheykhan, M. (2021). Toxicological effects of Ag_2O and Ag_2CO_3 doped TiO_2 nanoparticles and pure TiO_2 particles on zebrafish (Danio rerio). *Chemosphere*, *263*. https://doi.org/10.1016/j.chemosphere.2020.128182

Malakar, A., Kanel, S. R., Ray, C., Daniel, D., & Nadagouda, M. N. (2020). 1 P re. *Science of the Total Environment*, 143470. https://doi.org/10.1016/j.scitotenv.2020.143470

Mishra, T., Hait, J., Aman, N., Jana, R. K., & Chakravarty, S. (2007). Effect of UV and visible light on photocatalytic reduction of lead and cadmium over titania based binary oxide materials. *Journal of Colloid and Interface Science, 316*(1), 80–84. https://doi.org/10.1016/j.jcis.2007.08.037

Mo, Y., Gu, A., Tollerud, D. J., & Zhang, Q. (2016). *Nanoparticle toxicity and environmental impact*. Elsevier Inc. https://doi.org/10.1016/B978-0-12-803269-5.00005-X

Mohan, S., & Gandhimathi, R. (2009). Removal of heavy metal ions from municipal solid waste leachate using coal fly ash as an adsorbent. *Journal of Hazardous Materials, 169*(1–3), 351–359. https://doi.org/10.1016/j.jhazmat.2009.03.104

Murruni, L., Leyva, G., & Litter, M. I. (2007). Photocatalytic removal of Pb(II) over TiO_2 and Pt-TiO_2 powders. *Catalysis Today, 129*(1-2 SPEC. ISS.), 127–135. https://doi.org/10.1016/j.cattod.2007.06.058

Parrino, F., Bellardita, M., García-López, E. I., Marcì, G., Loddo, V., & Palmisano, L. (2018). Heterogeneous photocatalysis for selective formation of high-value-added molecules: Some chemical and engineering aspects. *ACS Catalysis, 8*(12), 11191–11225. https://doi.org/10.1021/acscatal.8b03093

Peter, A., Indrea, E., Mihaly-Cozmuta, A., Mihaly-Cozmuta, L., Nicula, C., Tutu, H., & Bakatula, E. (2012). Dual efficiency of nano-structured TiO_2/zeolyte systems in removal of copper (II) and lead (II) ions from aqueous

solution under visible light. *AIP Conference Proceedings, 1425*(Ii), 139–143. https://doi.org/10.1063/1.3681986

Rosin-Paumier, S., Touze-Foltz, N., & Pantet, A. (2011). Impact of a synthetic leachate on permittivity of GCLs measured by filter press and oedopermeameter tests. *Geotextiles and Geomembranes, 29*(3), 211–221. https://doi.org/10.1016/j.geotexmem.2010.11.001

Sabour, M. R., & Amiri, A. (2017). Comparative study of ANN and RSM for simultaneous optimization of multiple targets in Fenton treatment of landfill leachate. *Waste Management, 65*, 54–62. https://doi.org/10.1016/j.wasman.2017.03.048

Sahar, A., Ali, S., Hussain, T., Jahan, N., & Zia, M. A. (2018). Efficient optimization and mineralization of UV absorbers: A comparative investigation with Fenton and UV/H_2O_2. *Open Chemistry., 2018*(16), 702–708.

Sarteep, Z., Pirbazari, A. E., & Aroon, M. A. (2016). Silver doped TiO_2 nanoparticles: Preparation, characterization and efficient degradation of 2,4-dichlorophenol under visible light. *Nanotechnology Journal of Water and Environmental Nanotechnology*, *1*(12). https://doi.org/10.7508/jwent.2016.02.007

Satyro, M. A., & Carroll, J. J. (2014). Phase equilibrium in the systems hydrogen sulfide+ methanol and carbon dioxide+ methanol. *Gas Injection for Disposal and Enhanced Recovery*, 99–110.

Show, P. L., Pal, P., Leong, H. Y., Juan, J. C., & Ling, T. C. (2019). A review on the advanced leachate treatment technologies and their performance comparison: An opportunity to keep the environment safe. *Environmental Monitoring and Assessment*, *191*(4). https://doi.org/10.1007/s10661-019-7380-9

Sobhanardakani, S., Jafari, A., Zandipak, R., & Meidanchi, A. (2018). Removal of heavy metal (Hg(II) and Cr(VI)) ions from aqueous solutions using Fe_2O_3@SiO_2 thin films as a novel adsorbent. *Process Safety and Environmental Protection, 120*(Ii), 348–357. https://doi.org/10.1016/j.psep.2018.10.002

Spasiano, D., Marotta, R., Malato, S., Fernandez-Ibañez, P., & Di Somma, I. (2015). Solar photocatalysis: Materials, reactors, some commercial, and pre-industrialized applications. A comprehensive approach. *Applied Catalysis B: Environmental, 170–171*, 90–123. https://doi.org/10.1016/j.apcatb.2014.12.050

Sreekantan, S., MohdZaki, S., Lai, C. W., & Wah Tzu, T. (2014). Post-annealing treatment for Cu-TiO_2 nanotubes and their use in photocatalytic methyl orange degradation and Pb(II) heavy metal ions removal. *EPJ Applied Physics, 67*(1), 1–8. https://doi.org/10.1051/epjap/2014130453

Strauss, A., Reyneke, B., Waso, M., & Khan, W. (2018). Compound parabolic collector solar disinfection system for the treatment of harvested rainwater. *Environmental Science: Water Research & Technology*. https://doi.org/10.1039/C8EW00152A

Subramonian, W., Wu, T. Y., & Chai, S. (2017). Photocatalytic degradation of industrial pulp and paper mill effluent using synthesized magnetic Fe2O3 -TiO2: Treatment efficiency and characterizations of reused photocatalyst. *Journal of Environmental Management, 187*, 298–310. https://doi.org/10.1016/j.jenvman.2016.10.024

Taghavi, S. M., Momenpour, M., Azarian, M., Ahmadian, M., Souri, F., Taghavi, S. A., Sadeghain, M., & Karchani, M. (2013). Effects of nanoparticles on the environment and outdoor workplaces. *Electronic Physician, 5*(4), 706–712. https://doi.org/10.14661/2013.706-712

Tanveer, M., & Tezcanli, G. (2013). Solar assisted photo degradation of wastewater by compound parabolic collectors : Review of design and operational parameters. *Renewable and Sustainable Energy Reviews, 24*, 534–543. https://doi.org/10.1016/j.rser.2013.03.053

Varank, G., YaziciGuvenc, S., Gurbuz, G., & OnkalEngin, G. (2016). Statistical optimization of process parameters for tannery wastewater treatment by electrocoagulation and electro-Fenton techniques. *Desalination and Water Treatment, 57*(53), 25460–25473. https://doi.org/10.1080/19443994.2016.1157042

Wahyuni, E., Aprilita, N., Hatimah, H., Wulandari, A., & Mudasir, M. (2015). Removal of toxic metal ions in water by photocatalytic method. *American Chemical Science Journal, 5*(2), 194–201. https://doi.org/10.9734/acsj/2015/13807

Wang, X. (2012). Nanomaterials as sorbents to remove heavy metal ions in wastewater treatment. *Journal of Environmental & Analytical Toxicology*, *02*(07). https://doi.org/10.4172/2161-0525.1000154

Yang, J. K., & Lee, S. M. (2005). EDTA effect on the removal of Cu(II) onto TiO_2. *Journal of Colloid and Interface Science, 282*(1), 5–10. https://doi.org/10.1016/j.jcis.2004.08.162

Yeber, M. C., Soto, C., Riveros, R., Navarrete, J., & Vidal, G. (2009). Optimization by factorial design of copper (II) and toxicity removal using a photocatalytic process with TiO_2 as semiconductor. *Chemical Engineering Journal, 152*(1), 14–19. https://doi.org/10.1016/j.cej.2009.03.021

Zangeneh, H., Zinatizadeh, A. A., Feyzi, M., Zinadini, S., & Bahnemann, D. W. (2018). Application of a novel triple metal-nonmetal doped TiO2 (K-B-N-TiO2) for photocatalytic degradation of Linear Alkyl Benzene (LAB) industrial wastewater under visible light. *Materials Science in Semiconductor Processing, 75*(September 2017), 193–205. https://doi.org/10.1016/j.mssp.2017.11.040

Zhao, D., & Wu, X. (2018). Nanoparticles assembled SnO2 nanosheet photocatalysts for wastewater purification. *Materials Letters, 210*(September), 354–357. https://doi.org/10.1016/j.matlet.2017.09.068

Zheng, P., Pan, Z., Li, H., Bai, B., & Guan, W. (2015). Effect of different type of scavengers on the photocatalytic removal of copper and cyanide in the presence of TiO_2@ yeast hybrids. *Journal of Materials Science: Materials in Electronics, 26*(9), 6399–6410. https://doi.org/10.1007/s10854-015-3229-3